

A Comparison of Anthracene  
and Phenanthrene in Coal Liquefaction

K. C. Kwon

Chemical Engineering Department  
School of Engineering and Architecture  
Tuskegee Institute, Alabama 36088

INTRODUCTION

A comparison of anthracene and phenanthrene was made by liquefying either Wyodak coal or Kentucky 9/14 coal in the presence of either hydrogen or nitrogen. 1-methylnaphthalene (1-MN) was employed as a physical solvent. Reaction products are separated into a tetrahydrofuran (THF)-soluble fraction, a preasphaltene fraction, an asphaltene fraction and an oil-plus-gas-plus water fraction.

EXPERIMENTS

A series of reactions were conducted in a 25 cc, 316 stainless steel micro-reactor to liquefy either Wyodak coal or Kentucky 9/14 coal under the various operation conditions. Another series of reactions were performed in a 50 cc flask to dissolve either Wyodak coal or Kentucky 9/14 coal with either neat aromatic compounds such as anthracene and phenanthrene, or mixtures of neat aromatics and their dihydroaromatics under the atmospheric pressure. The reaction product is separated by using a pressure filtration procedure. Conversions of aromatics into hydroaromatics are analyzed by using a gas chromatograph. Coal conversions are calculated on a moisture-and-ash-free-coal basis.

DISCUSSION

Both anthracene and phenanthrene are converted more into their hydroderivatives in the presence of Kentucky 9/14 coal than in the presence of Wyodak coal. This fact may suggest that minerals in Kentucky 9/14 coal act as more active catalysts than minerals in Wyodak coal in hydrogenating aromatics such as anthracene and phenanthrene in the presence of molecular hydrogen (Table 1).

Wyodak coal is converted more into an oil-water-gas fraction in the presence of anthracene than in the presence of phenanthrene, while producing the same amount of preasphaltene plus asphaltene in the presence of either anthracene or phenanthrene. Therefore, anthracene and its derivatives are to some degree better solvents than phenanthrene and its derivatives in liquefying Wyodak coal (Table 1).

The conversion of Kentucky 9/14 coal is influenced more by hydrogen pressure than the conversion of Wyodak coal in the presence of either anthracene or phenanthrene (Table 1). This fact suggests that molecular hydrogen may play a more dominant role than hydroaromatics in liquefying Kentucky 9/14 coal or that the minerals in Kentucky 9/14 coal are actively hydrogenating the aromatic solvent. The analysis of the oil fraction suggests the latter.

The conversion of both anthracene and phenanthrene to dihydroderivatives increases as the initial hydrogen pressure increases. The conversion of Wyodak coal increases from 44 % to 58 % and the hydrogenation of anthracene increases from 6 % to 17 % in the presence of anthracene, whereas the conversion of Wyodak coal increases from 40 % to 48 % and the hydrogenation of phenanthrene does not increase by increasing the initial hydrogen pressure from 500 psig to 1100 psig (Table 1). These facts show that anthracene is readily hydrogenated and its derivatives are better hydrogen donors or shuttlers than phenanthrene and its derivatives in liquefying Wyodak coal.

The conversion of Ky 9/14 coal is 42.4 % and the hydrogenation of anthracene is 4.4 % in the presence of nitrogen (Table 1). The conversion of Ky 9/14 coal is 38 % and no hydrogenation of phenanthrene is observed in the presence of nitrogen. This fact demonstrates that anthracene is more active than phenanthrene

in liquefying Ky 9/14 coal in the absence of hydrogen, by extracting hydrogen from coal to be converted into dihydroanthracene and then breaking down coal structure.

Conversions of Ky 9/14 coal and anthracene to hydroanthracenes are 72.4 % and 17.6 % respectively in the presence of 500 psig hydrogen, while conversions of Ky 9/14 coal and phenanthrene are 75.3 % and 0 % respectively in the presence of 500 psig hydrogen, in spite of the fact that more hydrogen donor is available in the former case (Table 1). Preasphaltene-plus-asphaltene fraction is 53 % in the presence of anthracene and 500 psig hydrogen, whereas preasphaltene-plus-asphaltene fraction is 46 % in the presence of phenanthrene and 500 psig hydrogen. This fact may indicate that either solubility of Ky 9/14 coal in phenanthrene and its derivatives is inherently better than in anthracene and its derivatives, or that dihydroanthracene may be undergoing extensive retrogressive reaction with coal or itself, producing more preasphaltene-plus-asphaltene fraction. This evidence may also suggest that the transfer rate of labile hydrogen from coal to anthracene is much faster than that of molecular hydrogen from the gaseous phase to liquid anthracene during the very early reaction stage due to low hydrogen pressure.

A series of runs were carried out to understand solvent quality on conversion of Wyodak coal in the presence of hydrogen, as shown in Run 3, Run 4 and Run 44 in Table 2. Conversions of coal in the presence of anthracene and its derivative is considerably higher than in the presence of either phenanthrene or 1-MN, where conversion of anthracene is 22.2 % as shown in Run 3. This indicates that a good hydrogen donor solvent may play a more dominant role than molecular hydrogen in liquefying Wyodak coal and that the solvent power of 1-MN is better than that of phenanthrene in the presence of hydrogen for the liquefaction of Wyodak coal.

Another series of runs were conducted to determine solvent quality on the liquefaction of Wyodak coal in the presence of nitrogen as shown in Run 45, Run 48 and Run 49 in Table 2. Conversion of Wyodak coal is higher in the presence of phenanthrene than in the presence of anthracene in the absence of hydrogen. This fact may demonstrate that phenanthrene is a better physical solvent than anthracene in the absence of hydrogen in the liquefaction of Wyodak coal, suggesting that it is the ease of hydrogenation of anthracene and the excellent H-donor behavior of its hydroderivatives that makes anthracene a good solvent in the presence of hydrogen.

Conversion of coal in the presence of anthracene is higher than that of phenanthrene at the reaction temperature of both 350 °C and 425 °C. Phenanthrene is not hydrogenated at 350 °C or 425 °C, but hydrogenations of anthracene are 2.6 % at 350 °C and 4.4 % at 425 °C (Table 2). The difference in coal conversion between anthracene and phenanthrene is less significant at lower reaction temperature. This fact suggests that less labile hydrogen from coal to anthracene is transferred at the lower temperature and the inherent solvent power of the vehicle used is important.

A series of experiments were carried out by liquefying coal with neat aromatic compounds or mixtures of neat aromatic compounds and their hydroderivatives at their boiling temperature under the atmospheric environment (Table 3). Conversion of Wyodak coal in the presence of phenanthrene is higher than in the presence of anthracene, where no hydrogenation of both anthracene and phenanthrene was observed. This fact shows that the solubility of Wyodak coal in phenanthrene is higher than in anthracene under the atmospheric environment and in the absence of other solvents.

Conversion of Ky 9/14 in the presence of phenanthrene is higher than in the presence of anthracene, where hydrogenation of both phenanthrene and anthracene was not observed as shown in Run 19 and Run 22 in Table 3. On the other hand, the conversion of Ky 9/14 coal in the presence of phenanthrene is lower than in the presence of anthracene at 350 °C under 2000 psig nitrogen pressure, as shown in Run 40 and Run 41 in Table 2. This fact suggests that either labile hydrogen does not react with anthracene or escapes into the atmosphere before reacting with anthracene due to the low pressure, whereas labile hydrogen reacts with

anthracene at high pressure. The conversion of Ky 9/14 coal in the presence of a mixture of phenanthrene and dihydrophenanthrene is higher than in the presence of a mixture of anthracene and dihydroanthracene, and the conversion of dihydrophenanthrene is higher than that of dihydroanthracene, as shown in Run 23 and Run 24 in Table 3. On the other hand, the effect of dihydroanthracene on the increment of coal conversion, as shown in Run 19 and Run 23 in Table 3 is higher than the effect of dihydrophenanthrene on the increment of coal conversion, as shown in Run 22 and Run 24 in Table 3. This fact again suggests that dihydroanthracene is a better hydrogen donor solvent than dihydrophenanthrene. Neat anthracene is a poorer solvent than neat phenanthrene (about 1/3) for both Wyodak coal and Ky 9/14 coal at 330 °C. But when 20 % of the dihydrocompound is present, the anthracene compound mixture is a better solvent than the phenanthrene mixture. With Ky 9/14 coal, the phenanthrene is the best solvent, neat and in the presence of the dihydrocompound.

The disappearance of the dihydrocompounds is in agreement with the liquefaction of coal. In the presence of Ky 9/14 coal, dihydrophenanthrene is lost most rapidly, whereas in the presence of Wyodak coal, dihydroanthracene is lost most rapidly (Table 3).

A series of reactions were performed in the presence of neat aromatic compounds and 1100 psig nitrogen (initial) as shown in Table 4. The conversions of Ky 9/14 coal are 32 % in the presence of anthracene and 51 % in the presence of phenanthrene whereas the conversions of Wyodak coal are 33 % in the presence of anthracene and 43 % in the presence of phenanthrene. These data also show that neat phenanthrene is a better physical solvent than neat anthracene in liquefying both Wyodak coal and Ky 9/14 coal in the absence of hydrogen.

Another series of runs with Ky 9/14 coal were compared in the absence of hydrogen in terms of initial nitrogen pressure, as shown in Table 1. The conversions of Ky 9/14 coal are 42 % in terms of the THF soluble fraction and 29 % in terms of the preasphaltene-plus-asphaltene fraction at the 1100 psig initial nitrogen pressure, whereas the conversions of Ky 9/14 coal are 39 % and 24 % respectively at the zero psig initial nitrogen. The closeness of the values for dihydroanthracene formed suggests that the conversion and product distribution would also be similar. The only firm conclusion is that pressure helps total liquefaction and seems to hint oil-water-gas formation. Anthracene is a better solvent than phenanthrene under these conditions.

#### CONCLUSIONS

The relative behavior of phenanthrene and anthracene depends on whether the solvents are compared neat or in the presence of other solvents, upon the gaseous environment, and upon the coal. When anthracene is the better solvent, conditions appear to favor the formation of dihydroanthracene which is an excellent hydrogen donor. When phenanthrene is the better solvent, the inherently better solvent power of phenanthrene itself for that coal appears to be the dominant factor. The minerals in the coal, and possibly the coal itself, are also important in determining the preferred solvent.

#### REFERENCES

1. Appell, H. R. "The Effect of Solvent Composition on Product Distribution." Unpublished, Pittsburgh Energy Technology Center.
2. Curtis, C. W., J. A. Guin, and K. C. Kwon. "Coal and Solvolysis in a Series of Model Compound System." Presented to the AIChE Annual Meeting, November, 1982, Los Angeles.
3. Curtis, C. W., J. A. Givin, K. C. Kwon, and N. L. Smith. "Selectivity of Coal Minerals Using Cyclohexane as a Probe Reactant." Fuel (In Press), London, England.
4. Derhyshire, F. J. and D. D. Whitehurst. "The Influence of Polyaromatic Solvent Components on Coal Liquefaction." Proceedings on the Fifth Annual EPRI Contractor's Conference on Coal Liquefaction, p. 9-1, 1980.
5. Gangwar, T. E. and H. Prasad. "Hydrogen-Transfer Catalytic Activity of Minerals Common to Coal." Fuel, 58, p. 577, London, England, 1979.
6. Garg, D. and E. N. Givens. "Pyrite Catalysis in Coal Liquefaction." Ind. Eng. Chem. Process Design and Development, 21, p. 113, 1982.
7. Guin, J. A., C. W. Curtis, and K. C. Kwon. "Pyrite Catalyzed Coal Liquefaction Using Quinoline/Tetrahydroquinoline as a H-Donor System." Fuel, In Press, London, England, 1983.
8. Jackson, W. R., F. P. Larkins, M. Marshall, D. Rash, and N. White. "Hydrogenation of Brown Coal. 1. The Effects of Additional Quantities of the Inorganic Constituents." Fuel, 58, p. 281, London, England, 1979.
9. Lytle, J. M., R. E. Wood, and W. H. Wisler. "Kinetics of Coal Liquefaction: Effect of Catalyst, H<sub>2</sub> Concentration and Coal Type." Fuel, 59, p. 471, London, England, 1980.
10. Mochida, I., A. TaKarabe, and K. Takeshita. "Solvolytic Liquefaction of Coals with a Series of Solvents." Fuel, 58, p. 17, London, England, 1979.
11. Neavel, R. C. "Exxon Donor Solvent Liquefaction Process." Phil. Trans. Royal Society, London, A 300, p. 141, London, England, 1981.
12. Padrick, T. D., A. W. Lynch and H. P. Stephens. "Effect of Solvent on the Dissolution of Wyodak Coal." Proceedings of the Department of Energy Integrated Two-Stage Liquefaction Meetings, p. 6-2, Albuquerque, New Mexico, October, 1982.
13. Rottendorf, H. and M. A. Wilson. "Effects of In-Situ Mineral Matter and a Nickel-Molybdenum Catalyst on Hydrogenation of Lidell Coal." Fuel, 59, p. 175, London, England, 1980.
14. Utz, B. R., H. R. Appell and B. D. Blaustein. "Vehicle Studies in Short Contact Time Liquefaction." Proceedings of the Department of Energy Integrated Two-Stage Liquefaction Meetings. p. 7-1, Albuquerque, New Mexico, October, 1982.
15. Utz, B. R., Narain, N. K., Appell, H. R. and Blaustein, B. D. "Solvent Analysis of Coal Derived Products, Using Pressure Filtration," Am. Chem. Soc. Symp. Ser., edited by Fuller, American Chemical Society, Washington, D. C., 1982.

Table 1 - Effects of Hydrogen Pressure on Coal Conversions for 15 min. at 425 °C

RUN NO.	45	1	3	2	4	37*	9	6	38*	10	7	47**
Hydrogen Charge at the Room Temperature (psig)	0	500	1100	500	1100	0	500	1100	0	500	1100	0
1 gm Aromatics plus 4 g 1-MN	-	+	-	+	-	+	+	+	-	+	-	+
Anthracene	-	-	-	+	-	-	-	-	+	-	+	-
Phenanthrene	-	-	-	+	-	-	-	-	+	-	+	-
Type of Coal	+	+	+	+	+	-	+	-	-	-	-	-
Wyodak	-	-	-	-	-	+	+	+	+	+	+	+
Ky 9/14	-	-	-	-	-	-	-	-	-	-	-	-
Coal Conversion (wt %)	36.1	44.3	57.7	40.3	47.9	42.4	72.4	83.8	37.7	75.3	84.7	39.5
THF Soluble	-	-	-	-	-	11.0	26.3	26.9	13.4	21.0	27.6	10.0
Preasphaltene	-	-	-	-	-	18.1	26.5	33.6	14.9	25.1	30.0	13.9
Asphaltene	8.0	14.0	12.6	11.6	10.6	29.1	52.7	60.5	28.3	46.2	57.6	23.9
Preasphaltene plus Asphaltene	28.2	30.3	45.1	28.7	37.3	13.2	19.7	23.2	9.5	29.1	27.0	15.6
Oil, Water and Gas												
Conversion of Aromatics (wt %)	NA	6.4	16.9	0	0	4.4	17.6	28.4	0	0	3.8	4.5
Conversion to Dihydroaromatics	NA	93.6	77.2	100	100	95.6	71.7	50.7	100	100	95.3	95.5
Unconverted Aromatic												

\* 1100 psig initial nitrogen pressure at the room temperature

\*\* 14.7 psig initial nitrogen pressure at the room temperature

Table 2 - Conversions of Coals under the Various Reaction Conditions and for 15 min. at 425 °C

RUN NO.	3	4	6	7	37	38	40 <sup>**</sup>	41 <sup>**</sup>	42 <sup>*</sup>	44 <sup>*</sup>	45 <sup>*</sup>	46 <sup>*</sup>	48	49
<u>Type of Coal (i. g)</u>														
Wyodak	+	+	-	-	-	-	-	-	-	+	+	-	+	+
Ky 9/14	-	-	+	+	+	+	+	+	+	-	-	+	-	-
<u>1 g Aromatic Plus</u>														
4 g 1-MN	-	+	+	-	+	+	+	+	-	-	-	-	+	+
Anthracene	+	-	-	+	-	+	-	-	-	-	-	-	-	-
Phenanthrene	+	-	-	+	-	+	-	-	-	-	-	-	-	+
<u>Gas Charge at the Room Temperature (1100 psig)</u>														
Hydrogen	+	+	+	+	-	+	-	-	+	+	-	-	+	+
Nitrogen	-	-	-	-	+	+	+	+	-	-	+	+	-	+
<u>Coal Conversion (wt %)</u>														
THF Soluble	57.7	47.9	83.8	84.7	42.4	37.7	30.1	27.9	84.5	51.2	36.1	39.8	37.1	39.5
Preasphaltene	-	-	26.9	27.6	11.0	13.4	11.6	15.7	21.3	-	-	7.6	-	-
Asphaltene	-	-	33.6	30.0	18.1	14.9	13.7	12.6	31.2	-	-	16.4	-	-
Preasphaltene plus Asphaltene	12.6	10.6	60.5	57.6	29.1	28.3	25.3	27.9	52.4	14.1	8.0	23.9	8.6	9.1
Oil, Water and Gas	45.1	37.3	23.2	27.0	13.2	9.5	4.9	0	32.1	37.1	28.2	15.9	28.5	30.4
<u>Conversion of Aromatics (wt %)</u>														
Conversion to Dihydroaromatics	16.9	0	28.4	3.8	4.4	0	2.6	0	NA	NA	NA	NA	NA	3.3
Unconverted aromatic	77.8	100	50.7	95.3	95.7	100	97.4	100	NA	NA	NA	NA	NA	96.8

\* 5 g 1-Methylnaphthalene introduced in the absence of aromatics

\*\* 350 °C of reaction temperature

Table 3 - Effects of Aromatic Compounds and Dihydroaromatic Compounds on Coal Conversion at the Atmospheric Pressure and in the Absence of 1-Methylnaphthalene

<u>RUN NO.</u>	5	8	11	12	19	22	23	24
<u>Type of Coal</u>								
Wyodak	+	+	+	+	-	-	-	-
Ky 9/14	-	-	-	-	+	+	+	+
<u>Aromatics</u>								
10 g Anthracene	+	-	-	-	+	-	-	-
10 g Phenanthrene	-	+	-	-	-	+	-	-
8 g Anthracene plus	-	-	-	-	-	-	-	-
2 g Dihydroanthracene	-	-	+	-	-	-	+	-
8 g Phenanthrene plus	-	-	-	+	-	-	-	+
2 g Dihydrophenanthrene	-	-	-	-	-	-	-	-
Temperature (°C)	339	335	340	330	336	334	333	329
<u>Coal Conversion (wt %)</u>								
THF Soluble	6.5	18.3	51.8	21.6	9.8	32.6	37.3	45.8
Preasphaltene	2.2	1.0	2.3	1.4	6.2	7.2	19.4	15.8
Oil, Water, Gas and Asphaltene	4.3	17.3	49.5	20.2	3.6	25.4	17.9	30.0
Conversion of Dihydroaromatic (wt %)	0	0	36.3	18.9	0	0	14.8	26.0

Table 4 - Effects of Neat Aromatic Compounds at 425 °C  
and 15 min. on Coal Conversion in the Presence  
of 1100 psig Nitrogen at the Room Temperature  
and in the Absence of 1-Methylnaphthalene

<u>RUN NO.</u>	50	51	52	53
<u>Type of Coal (1 g)</u>				
Wyodak	-	-	+	+
Ky 9/14	+	+	-	-
<u>5 g Aromatics</u>				
Anthracene	+	-	+	-
Phenanthrene	-	+	-	+
<u>Coal Conversion (wt %)</u>				
THF Soluble	32.4	51.3	33.1	42.6
Preasphaltene	10.8	11.1	10.8	0.5
Asphaltene	8.8	14.0	6.7	14.1
Preasphaltene plus asphaltene	19.6	25.1	17.5	14.5
Oil, Water and Gas	12.8	26.1	15.7	28.1
<u>Conversion of Aromatic (wt %)</u>				
Conversion to Dihydroaromatic	0	0	2.7	0
Unconverted Aromatic	100	100	97.3	100

## THE EFFECT OF SHORT REACTION TIME ON THE LIQUEFACTION OF AN AUSTRALIAN BROWN COAL

M.G. Strachan<sup>A</sup>, N.R. Foster<sup>B</sup>, R.B. Johns<sup>A</sup> and R.S. Yost<sup>A</sup>

- A. Departments of Organic Chemistry and Chemical Engineering, University of Melbourne, Parkville, Victoria, Australia 3052.  
B. C.S.I.R.O. Division of Fossil Fuels, North Ryde, N.S.W., Australia 2113.

### INTRODUCTION

Short Reaction Time (SRT) liquefaction has attracted much research in recent years (1-11). The process, which involves dissolution of coal in a donor solvent during a short time domain, has many advantages over conventional longer reaction time systems. These include the consumption of negligible gaseous hydrogen, utilizing instead the inherent hydrogen in the coal via shuttling and aromatic transfer mechanisms (1,2). The design and mathematical modelling of continuous reactors is also facilitated by the knowledge of the behaviour of the coal at short residence times. The rapidity of the process has led to the development of two-stage liquefaction systems based on this new technology, thus enabling the decoupling of thermal from catalytic processes. Preliminary research on SRT systems has shown their potential to give significantly lower gas and higher liquid yields, hence enabling more efficient utilization of hydrogen in the liquefaction process.

The majority of the research has involved US bituminous coals, with Whitehurst (3) reporting that optimum oil yields are achieved with coals in the 77-87% CMAF range. He postulated the observed lower yields for the lower rank coals were a consequence of the insolubility of the initially formed fragments in the donor solvent due to their more polar nature. Other workers (12) have suggested the lack of rapid dissolution is a function of these coals having more alicyclic, rather than hydroaromatic and aromatic systems, and hence are less capable of internal hydrogen donation.

The liquefaction of an Australian bituminous coal, Liddell, at SRT conditions has recently been reported (9,10,11). The authors observed trends similar to those found for US bituminous coals, with significant conversion occurring within the first few minutes of reaction. To determine whether Australian low rank coals display similar SRT behaviour to their US counterparts a Victorian brown coal has been investigated. This paper reports the results of the study; emphasizing conversion, oil yields and product analyses.

The coal used for this study was a medium-light lithotype Victorian brown coal from the Loy Yang Field (bore 1277, depth 67-68 m). The dried coal (particle size range: 90-150  $\mu\text{m}$ ) was injected into the donor solvent, tetralin, at temperature. The SRT reactor and details of its operation are described elsewhere (10,11). The reaction temperature was 380°C, the solvent to coal ratio 6:1, and the hydrogen pressure after injection typically 2100-2350 psig. The reaction times investigated were: 0,2,3,4,10,20,45 and 120 minutes.

The Total Oils (defined as  $\text{CH}_2\text{Cl}_2$  solubles) and residues have been investigated and characterized by a variety of analytical and spectroscopic methods. This has enabled both physical and chemical insights into the reactions occurring during the initial and subsequent dissolution of the brown coal.

### RESULTS AND DISCUSSION

The product distribution data (Table 1) shows both the conversion and oil yields to increase with reaction time. Surprisingly, there is conversion at zero time, which is associated mainly with gas production as reflected in the very high gas/oil yield ratio. Gas analyses however show its composition to be overwhelmingly carbon oxides with only a minor portion of hydrocarbon gases. Similar gas compositions are observed at the other reaction times with only the absolute amounts of the gases varying. The general trend is to increasing gas yields with reaction time. Although  $\text{CO}_2$  and CO dominate the gas production at all reaction times, the hydrocarbon gases do not become significant until 20 minutes of reaction time. Prior to this they are only in trace amounts. The zero time conversion suggests that contact of the dried coal with the hot solvent for only a few seconds is sufficient to promote decarboxylation,

decarbonylation and to a much lesser extent dealkylation reactions. The oil yield at zero time may possibly arise from the easily extractable, non-covalently bonded material in the coal matrix as 3.47% of the coal is solvent extractable (14). Decomposition and dissolution of the coal structure is significant even at 3 minutes with conversions of greater than 20%.

The data indicate the existence of two distinct reaction time zones; the first being prior to 10 minutes and the second from this time. In the first few minutes of reaction there is much gasification as defunctionalization reactions of the coal matrix occur. This is markedly illustrated by both the gas yields and gas/oil yield ratios. The amount of water production is relatively constant indicating the major reaction processes are rupture of the weaker bonds in the coal structure rather than dehydroxylation and upgrading of solubilized species. However, in the second time zone gas production remains constant, with the gas/oil yield ratio actually decreasing, suggesting that gasification is now mainly dependent on the removal of alkyl substituents rather than carboxyl and carbonyl functional groups. These have been predominantly removed within the first few minutes of reaction. The water yield increases significantly as does the  $H_2O$ /oil yield ratio indicating the removal of hydroxyl moieties. These may arise either from dehydroxylation of the coal matrix to aid its dissolution or from the upgrading of the already solubilized fragments.

Donor solvent hydrogen consumption data also supports the concept of two separate reaction periods. As expected, little hydrogen is consumed during the initial stages of dissolution, where the removal of carboxyl and carbonyl groups, via gasification, is dominant. This low hydrogen consumption may be a direct result of the coal utilizing its inherent hydrogen by shuttling type mechanisms. Although consumption does increase with time, it is much greater during the latter reaction period. The hydrogen is required to stabilize radical species produced by both cleavage and more vigorous defunctionalization of the coal matrix.

The conversion value for 120 minutes is very similar to that reported (15) for the same coal hydrogenated under conventional batch autoclave conditions (56% cf. 60%), although the oil yields differ markedly (25% cf. 46%). This difference is difficult to rationalize and results from the much higher water and gas yields for the SRT experiment. The Loy Yang conversions and oil yields are lower than those reported for Liddell coal under similar conditions. The parallel between increasing water production and oil yield tends to give credence to Whitehurst's hypothesis that the lower oil yields at short times for low rank coals are due to the insolubility of the very polar initially formed fragments.

The elemental analyses of the residues (Table 2) shows increasing carbon and decreasing oxygen contents with increasing reaction time. The removal of heteroatom moieties is further evidenced by the O/C ratios which similarly decrease. The H/C ratios however decrease only slightly with time suggesting the difficulty of dealkylation reactions and hence the relative preservation of hydrogen in the residues. The similar H/C values for the various reaction times indicate the residues are mainly the result of loss of peripheral heteroatom functionalities and not subject to gross structural alteration such as forming polycondensed aromatic systems. If this were the case it would be reflected in a significant lowering of H/C values with time. The H/C ratio for the zero time residue is lower than for the parent coal confirming the instantaneous gasification and extraction of non-bound material. The general trends in the Total Oils are also decreasing oxygen and increasing carbon contents with time. This correlates with increasing H/C and decreasing O/C ratios, showing a loss of heteroatom functionality and a lowering of the condensed nature (16) of the oils with time. Again the data can be divided into two regions centered on 10 minutes, as demonstrated by the much lower H/C and O/C ratios after this time compared to those prior. This further implies the time dependency of different liquefaction processes.

The IR Spectra (Fig. 1) of the residues both qualitatively and semiquantitatively support the forementioned data. The hydroxyl absorption decreases only marginally in the first few minutes of reaction but more markedly at longer times. This corresponds with the observed water yields. Similarly the carbonyl

absorption decreases rapidly with time and correlates with the production of carbon oxides. Whitehurst (3) has observed for low rank coals a good correlation between the loss of oxygen and the formation of carbon dioxide and carbon monoxide. There is also proportionate increases in aromatic C=C stretching and C-H bending with time, suggesting the residues are acquiring greater aromatic character. The proportion of aliphatic C-H stretching and bending vibrations slightly increase with time paralleling the loss of heteroatom functionality. This further illustrates the relative inertness of alkyl compared to heteroatom functionalities, and supports the forementioned gas composition data.

The trends are not as well defined for the Total Oil (TO) (Fig. 2), with the hydroxyl absorptions although being proportionately larger (approx. 16%) varying little with time. This implies that the forementioned increased water production is more likely a result of cleavage and dissolution of the matrix rather than upgrading of the already solubilized species. There is a general decrease in the carbonyl absorptions with time, while the converse is observed for the aliphatic C-H stretchings. The aromatic C-H bending, although a large percentage at 2 minutes (approx. 15%) decreases rapidly to a constant value (approx. 8%) from 4 minutes onwards. This is generally at the expense of increasing aromatic C=C and aliphatic C-H stretchings.

CP-MAS  $^{13}\text{C}$  nmr of the residues (Fig. 3) further illustrates the significant reactivity of the coal at SRT. The aromaticity,  $f(a)$ , increases dramatically after only 2 minutes reaction from 0.61 in the parent coal to 0.78 in the residue. Even at zero time  $f(a)$  is 0.63, reflecting the loss of carboxyl and carbonyl groups as gases. The  $f(a)$  values increase only marginally from 0.78 to 0.83 with time, supporting earlier conclusions from elemental analyses that all the residues have similar aromatic structure, differing mainly in degree of functionality.

$^1\text{H}$  nmr and structural parameters derived from Brown-Ladner equations (Table 3) give additional information on the nature of the TO. The percentage of exchangeable protons  $[H(\text{exch})]$  increases with time, showing an increasing proportion of phenolic groups in the oils. This trend was not as evident from IR data. The values for  $H(\text{exch})$  further suggest two reaction time zones as they cluster into two discrete groups. Although there are no discernable trends with the percentage of aromatic protons ( $H_{ar}$ ), the percentage of protons on carbons  $\beta$  and further from aromatic rings ( $H_0$ ) tend to increase with time. This is also shown in the values for the average chain length ( $n$ ). The oil produced at zero time has both the greatest proportion of  $H_0$  and the largest value of  $n$ , suggesting it is only the solvent extractable material from the coal. Solvent extracts of a Victorian brown coal of the same lithotype have been observed to contain a significant amount of straight chain material, either as alkanes, alcohols or fatty acids (17). The value of  $n$  then decreases to a minimum at 10 minutes and increases to 120 minutes; indicating more complete decomposition of the coal in this longer time domain. The increased chain lengths could result from cleavage of alicyclic systems. The aromaticity,  $f(a)$ , and degree of aromatic substitution,  $\sigma$ , generally decrease with increasing reaction time. The trends for the parameter  $\frac{H_{ar}}{C_{ar}}$ , i.e., the degree of condensation, are not as clearly defined, but it appears to increase with time implying smaller size aromatic systems. The decrease in aromaticity and substitution of the oil implies that either some upgrading of the initially solubilized material has occurred or the later dissolved material was more defunctionalized prior to dissolution. More likely it is a combination of both processes.

The Molecular Weights (MW) of the Total Oil (Table 3) are all similar with the number average MW ( $M_n$ ) varying from 210-320 with no readily identifiable trend with time. The values of  $M_n$  are low compared to that reported for an oil produced from the same coal under normal batch autoclave conditions ( $M_n = 487$ ). The weight average MW ( $M_w$ ) and MW distribution (MWD) also show no apparent trends. These observations are most likely a direct consequence of the insolubility of a large portion of the oils in the solvent, THF, used for MW determination. Hence only smaller MW species from the very heterogeneous Total Oil have been selectively dissolved. This insolubility may be itself indicative of the high MW of these Total Oils.

Pyrolysis-Gas Chromatography of the residues (Fig. 4) reveals a major

reduction of aliphatic components within the first 4 minutes of reaction, and with only alkyl phenols and catechols remaining after 45 minutes. This indicates that the more easily accessible and removable aliphatic material is extracted preferentially from the coal matrix in the initial stages of dissolution, while at longer times the coal structure itself must be more severely decomposed to increase the oil yield. This is also revealed by the decrease in the percentage of residue pyrolysed. The presence of phenolic species is directly relatable to the lignin input to the brown coal. Their existence in the pyrograms of the residues from 20 and 45 minutes supports the hypothesis that further oil production results from cracking of the lignin-type components of the coal macromolecules. Pyrolysis-Gas Chromatograms of the TOs, which are in effect simulated distillation profiles, all appear very similar. They differ quantitatively rather than qualitatively in composition.

The residues were degradatively oxidized by peroxytrifluoroacetic acid, a technique known as Deno Oxidation (18). It selectively oxidizes aromatic rings and leaves the aliphatic portion essentially intact. The data (Table 4) reveals that even at 0 minutes there is a marked reduction in the total yield of aliphatic hydrogen (65.6% cf 54.3%) compared to the parent coal from both assignable and unassignable material. Overall there is a reduction with time for both the total aliphatic and total spectrum hydrogen yields, suggesting the residues are becoming more aromatic in nature. Acetic acid (derived from aryl methyl groups) varies little with time suggesting little increase in dealkylation reactions. Succinic acid (derived from hydroaromatic structures) well illustrates the existence of two reaction zones. It is much reduced in the second due to both a possible internal hydrogen donation and a more severe rupture of the coal structure. Similarly, malonic acid (derived from bridging methylene groups) is also reduced in the second period as a result of bond cleavages and probably accompanying fragmentation of aromatic clusters. The 1° and 2° protons decrease in accord with the total aliphatic hydrogen, whereas the 3° protons vary little with time. However, the protons on carbons  $\alpha$  to carbonyl containing functional groups decrease significantly with time, paralleling the loss of the functional groups as carbon oxides. The data support earlier conclusions from other techniques.

This paper has reported the results of a donor solvent SRT study of a Victorian brown coal. Although oil yields and conversion are lower than for bituminous coals they show trends similar to those reported for USA low rank coals. The dissolution process appears to occur in two chemically and physically distinct phases. One primarily involves extraction of the coal and removal of carboxyl and carbonyl groups while the other involves a more severe disruption and decomposition of the coal matrix and removal of hydroxyl moieties. In both phases dealkylation is not a dominant reaction.

#### ACKNOWLEDGEMENT

M.G. Strachan acknowledges the award of a University of Melbourne Research Scholarship.

#### REFERENCES

1. Han, K.W. and Yen, C.Y., Fuel, 1979, 58, 779
2. Whitehurst, D.D. and Mitchell, T.O., in Liquid Fuels from Coal, Ed. Ellington, R.T., p. 153, Academic Press, N.Y., 1977.
3. Whitehurst, D.D., A.C.S. Symp. Ser., 1980, 139, 133
4. Farcasiu, M., A.C.S. Symp. Ser., 1981, 192, 151.
5. Longanbach, J.R., Droege, J.W. and Chauhan, S.P., A.C.S. Symp. Ser., 1980, 139, 165.
6. Kulik, C.J., Lebowitz, H.E. and Rovesti, W.C., A.C.S. Symp. Ser., 1980, 139, 193.
7. Heck, R.H., Mitchell, T.O., Stein, T.R. and Dabkowski, M.J., A.C.S. Symp. Ser., 1981, 139, 199.
8. Winnans, R.E., King, H.H., McBeth, R.L. and Botto, R.B., A.C.S. Div. Fuel Chem. Prepr., 1983, 28(5), 8.
9. Foster, N.R., Clark, K.N., Wilson, M.A. and Weiss, R.G., Proc. of the Symp. on the characterisation of Aust. Coal and their Consequences for Utilization p. 30-1, Sydney, May 1982.

10. Foster, N.R., Wilson, M.A., Weiss, R.G. and Clark, K.N., Ind. Eng. Chem. Prod. Res. Dev., 1983, in press
11. Foster, N.R., Weiss, R.G., Clark, K.N. and Young, M.M., Proc. Int. Conf. Coal Sci., p. 129, Pittsburgh, August 1983.
12. Reggel, L., Wender, I. and Raymond, R., Fuel, 1973, 52, 163.
13. Strachan, M.G., Johns, R.B. and Yost, R.S., J. Chromatog. Submitted for publication.
14. Strachan, M.G., McGavan, D.G. and Johns, R.B., Unpublished results.
15. Strachan, M.G., Vassallo, A.M. and Johns, R.B., A.C.S. Div. Fuel Chem. Prepr., 1983, 28(5), 226.
16. Curtis, C.S., Fuel, 1980, 59, 579.
17. Chaffee, A.L., Ph.D. Thesis, University of Melbourne, 1981.
18. Deno, N.C., Greigger, B.A. and Stroud, S.G., Fuel, 1978, 57, 455.

TABLE 1: PRODUCT DISTRIBUTION

Reaction Time (min)	Conversion %	Oil <sup>A</sup> yield	H <sub>2</sub> O <sup>A</sup> yield	Residue <sup>A</sup>	Gas <sup>A,B</sup>	H <sub>2</sub> O/oil yield	Gas/oil yield
0	9.0	0.90	2.59	91.00	5.50	2.88	6.12
2	12.61	5.12	2.04	87.39	5.45	0.40	1.06
3	21.02	6.08	2.43	78.98	12.51	0.40	2.06
4	27.53	7.63	2.89	72.47	17.01	0.38	2.23
10	32.39	10.65	4.77	67.61	16.91	0.45	1.59
20	39.91	18.08	7.17	60.09	14.66	0.40	0.81
45	48.95	19.55	15.32	51.05	14.08	0.78	0.72
120	56.28	25.92	15.96	43.72	14.40	0.62	0.56

A - g/100 g DAF Coal    B - By difference

TABLE 2: ELEMENTAL ANALYSES

Time (min)	C	H	O <sup>A</sup>	N	H/C	O/C <sup>A</sup>	N/C	Ash
LY 1277	62.35	5.20	31.89	0.59	1.00	0.38	0.01	0.71
<b>Total Oils</b>								
0	74.69	2.48	22.30	0.53	0.40	0.22	0.01	6.00
2	76.43	3.50	19.74	0.33	0.55	0.19	0.00	0.90
3	76.87	4.18	24.50	0.49	0.65	0.24	0.01	2.0
4	68.30	3.77	27.50	0.40	0.66	0.30	0.01	1.0
10	73.84	4.17	21.81	0.16	0.68	0.22	0.00	0.70
20	84.55	5.96	9.14	0.35	0.85	0.08	0.00	0.40
45	82.93	5.87	10.72	0.41	0.85	0.09	0.00	2.40
120	86.98	6.23	6.20	0.50	0.86	0.05	0.00	0.40
<b>Residues</b>								
0	65.24	4.68	29.44	0.65	0.86	0.34	0.01	0.79
2	67.28	4.62	27.39	0.71	0.82	0.31	0.01	0.12
3	68.86	4.62	25.78	0.73	0.81	0.28	0.01	1.13
4	69.35	4.62	25.29	0.74	0.80	0.27	0.01	1.06
10	70.51	4.70	24.06	0.79	0.80	0.26	0.01	1.06
20	72.16	4.70	22.37	0.83	0.78	0.23	0.01	1.06
45	74.40	4.87	19.79	0.95	0.79	0.20	0.01	1.97
120	75.71	5.03	18.23	1.01	0.79	0.18	0.01	2.29

A - Oxygen by difference

TABLE 3: <sup>1</sup>H NMR AND MW DATA ON TOTAL OILS

Time (min)	<sup>1</sup> H NMR DATA							MW DATA <sup>C</sup>				
	Ho	Ha	Har	H(exch)	Hali/Har	n= Ho/Hc +1	f(a) <sup>A</sup>	Haru/Car <sup>A</sup>	A <sub>o</sub>	Mn	Mw	MWD
0	61.9	15.7	22.4	N.D.	3.47	4.96	0.84	0.41	0.74	210	411	1.96
2	28.8	20.1	48.6	1.4	0.95	2.29	0.87	0.59	0.48	260	210	0.81
3	58.3	19.8	24.7	1.8	3.22	3.56	0.67	0.83B	0.61	295	432	1.46
4	31.8	26.6	38.8	1.9	1.51	2.20	0.79	0.88B	0.63	279	331	1.19
10	35.5	29.9	32.1	3.1	2.02	2.18	0.78	0.69	0.59	282	442	1.57
20	47.3	25.4	24.0	3.3	3.03	2.86	0.69	0.57	0.48	319	754	2.36
45	35.7	27.6	32.5	3.7	1.95	2.30	0.73	0.67	0.44	298	304	1.02
120	45.7	20.0	30.5	3.8	2.15	3.28	0.72	0.66	0.35	249	393	1.58

N.D. - Not Determined. A - Brown-Ladner Method. B - High oxygen content in sample.

C - GPC-HPLC method for molecular weight determination

TABLE 4: <sup>1</sup>H NMR SPECTRAL DATA OF (WT %) YIELD OF HYDROGEN APPEARING IN TFA<sup>A</sup> OXIDATION PRODUCTS

Time (min)	1° & 2° Protons (0.3-1.45 ppm)		3° Protons (1.45-2.20 ppm)		Protons α to acids and esters (2.20-3.45 ppm)		Total Aliphatic	Acetic Acid	Succinic Acid	Malonic Acid	Methanol	Total Spectrum	% Oxidized
	1° & 2°	3°	1° & 2°	3°	α	α							
LY 1277	18.2	17.0	18.4	18.4	53.6	6.5	3.8	1.3	0.4	65.6	98		
0	11.9	13.1	10.2	11.0	35.2	11.0	4.7	2.4	1.0	54.3	93		
2	10.1	9.1	9.5	10.8	28.7	10.8	3.2	2.0	2.7	47.4	98		
3	13.1	11.6	10.0	14.4	34.7	14.4	4.5	2.2	2.2	58.0	99		
4	13.2	11.0	8.7	14.0	32.9	14.0	4.0	2.0	2.2	55.1	98		
10	10.1	10.9	9.8	13.0	30.8	13.0	4.3	2.3	3.2	53.6	99		
20	11.2	11.3	7.1	12.0	29.6	12.0	2.7	0.7	3.2	48.2	97		
45	9.6	10.5	6.8	11.7	26.9	11.7	3.5	1.0	2.9	46.0	98		
120	6.5	9.5	5.2	11.7	21.2	11.7	3.0	0.8	0.7	37.4	95		

A - Peroxytrifluoroacetic acid

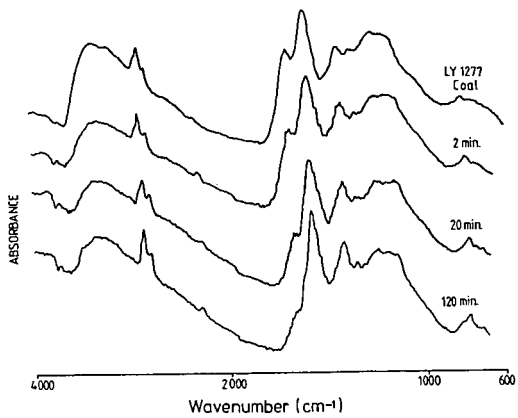


FIG. 1. IR SPECTRA OF LIQUEFACTION RESIDUES

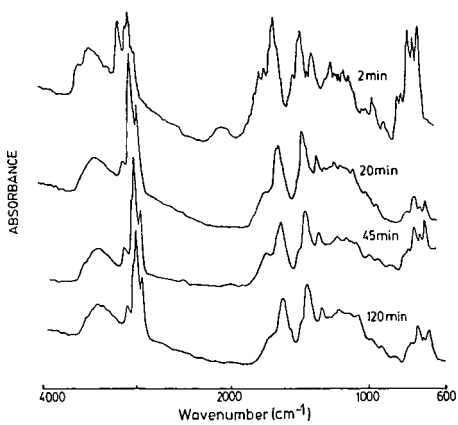


FIG. 2. IR SPECTRA OF TOTAL OILS

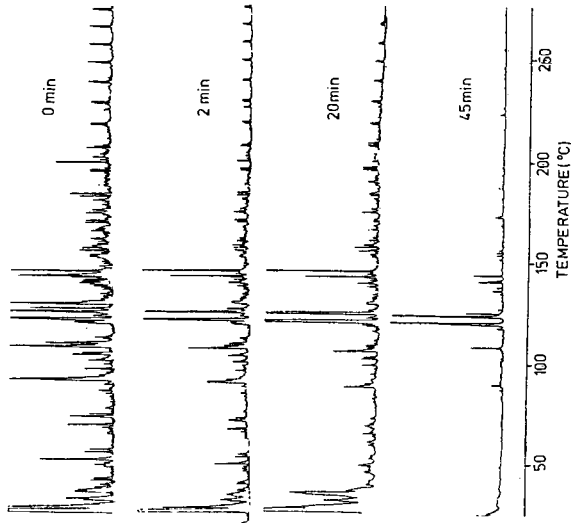
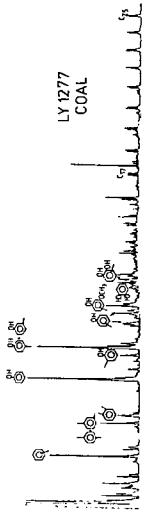


FIG. 4. PYROGRAMS OF LIQUEFACTION RESIDUES AND COAL

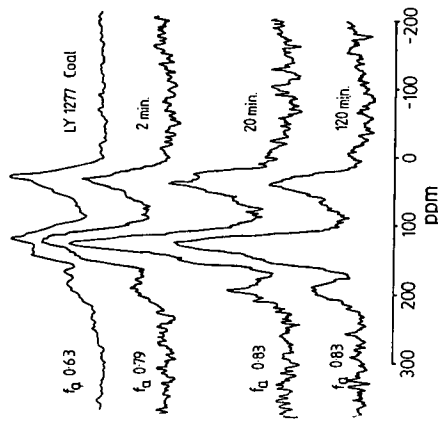


FIG. 3. CP-MAS  $^{13}C$  NMR SPECTRA OF LIQUEFACTION RESIDUES

## Combined Upgrading of Coal and Petroleum Residua

Christine W. Curtis, James A. Guin, Milo Pass, and Kan Joe Tsai

Chemical Engineering, Auburn University, Alabama 36849-3501

This investigation examines the feasibility of using heavy petroleum crudes and residua as solvents in coal liquefaction. The concept being explored is to determine if coal and heavy petroleum crudes and residua can be simultaneously processed with mutual upgrading of both materials. Previous work by Moschopedis and coworkers<sup>1-4</sup> has examined the liquefaction of coal using Athabasca oil sands bitumen, Lloydminster heavy oil, Coker gas oil and Cold Lake bitumen. The effectiveness of these materials as hydrogen donor solvents and their thermal stability under liquefaction conditions was also examined. The effects of process parameters on the production of reaction products was also investigated. Other investigations have been performed by Mochida and coworkers<sup>5</sup> in which several coals were liquefied in the presence of a Khafji vacuum residue. Other studies by Mochida<sup>6,7</sup> have included the liquefaction of an Australian brown coal in a prehydrogenated petroleum pitch and the liquefaction of subbituminous coals using pyrene and various Ashland pitches.

This study examines the conversion of a bituminous coal to soluble products through coprocessing with six heavy petroleum crudes and residua. These reactions were performed thermally, in an inert and in a hydrogen atmosphere, and catalytically in a hydrogen atmosphere. The petroleum materials used range from a whole crude to a variety of residua. Chemical and physical characterizations have been performed to determine what factors are most influential in producing the end product. To determine the sensitivity of coprocessing to reaction conditions and to determine the most optimal parameters, an evaluation of key reaction parameters has been performed.

### Experimental

Feedstock. Six petroleum crudes and residua, supplied by Cities Service Research and Development Company, have been examined for potential use as solvents for coal liquefaction processing. Analysis of the petroleum feedstocks are given in Table 1. The coals used in this study are a high volatile bituminous Illinois #6 coal, a Blacksville mine coal and a subbituminous coal, Clovis Point from Wyoming.

Screening Experiment. Screening experiments were performed at 400°C using a nitrogen atmosphere and a hydrogen atmosphere. Catalytic screening experiments with a hydrogen atmosphere were performed at 400° and 425°C. The equipment and reaction conditions used in these experiments were: a 50 cc stainless steel tubing bomb reactor, reaction time of 30 minutes, agitation at 860 cpm, and a solvent to coal ratio of 2:1. The reaction products were analyzed by a solvent separation scheme in which the product is successively extracted by pentane, benzene and methylene chloride/methanol. The liquid fractions obtained are oil (pentane solubles), asphaltenes (benzene soluble, pentane insolubles), and preasphaltenes (benzene insoluble, methylene chloride/methanol solubles), and insoluble organic matter. The weight of gases produced was also determined.

Parametric Evaluation. The reaction parameters evaluated as to their effect on coal conversion and product distributions from combined processing were reaction temperature, initial hydrogen reaction pressure, reaction time and diffusional pathlength of the catalyst. The reaction conditions for these evaluations are summarized below:

Reaction ConditionsParameter

	<u>Temperature</u>	<u>Pressure</u>	<u>Time</u>
Time	30 minutes	30 minutes	---
Temperature	----	425°C	425°C
Pressure	1250 psig H <sub>2</sub>	----	1250 psig
Agitation Speed	860 cpm	860 cpm	860 cpm
Coal	3 g, Illinois #6 or 3 g, Blacksville	3 g, Illinois #6	3 g, Illinois #6
Solvent	6 g, Maya Crude	6 g, Maya Crude	6 g, Maya Crude
Catalyst	None	1 g, Presulfided Shell 324 NiMo/Al <sub>2</sub> O <sub>3</sub> powdered (from 1/32" extrudates)	3 conditions were used: a. None Presulfided b. Shell 324 NiMo/Al <sub>2</sub> O <sub>3</sub> 1/16" extrudates c. Presulfided Shell 324 NiMo/Al <sub>2</sub> O <sub>3</sub> (from 1/16" extrudates)

The effect of thermal and catalytic combined processing on the reaction products from Clovis Point coal was also evaluated.

Characterization of the Petroleum Crudes and Residua. The petroleum crudes and residua were characterized by elemental analysis, molecular weight by vapor phase osmometry in pyridine, viscosity, Conradson Carbon, proton distribution, and specific gravity. Table 1 presents a composite of the physical and chemical characteristics of the petroleum crudes and residua.

Results and Discussion

Six heavy petroleum crudes and residua have been used as solvents in a series of coal liquefaction experiments to determine their ability to liquefy coal. The experiments were performed at 400° and 425°C using Illinois #6 coal and in three different environments: (1) a N<sub>2</sub> atmosphere, (2) a H<sub>2</sub> atmosphere and (3) and H<sub>2</sub> atmosphere using a pelletized presulfided NiMo/Al<sub>2</sub>O<sub>3</sub> catalyst.

Analyses of the solvents using a solubility extraction procedure developed for coal materials showed that the petroleum crudes were between ~80% to 90% soluble in pentane and the pentane insoluble materials were mostly benzene solubles, asphaltenes. The coal derived solvent CPDU-200A was ~85% pentane soluble with the remainder being asphaltenes. The petroleum solvents have hydrogen to carbon ratios of ~1.45 to 1.65 and sulfur contents between 2.8% and 4.6%.

Liquefaction in a Nitrogen Atmosphere. Liquefaction experiments were performed in a hydrogen deficient, nitrogen atmosphere to determine how readily the hydrogen-rich petroleum solvents could transfer hydrogen directly to coal, thereby converting coal to a soluble product. The ability of tetralin and coal-derived CPDU-200A to convert coal was also determined.

Coal conversion obtained using tetralin was 57.5%, by CPDU-200A was 51.5%, and the most converted by a petroleum crude was 36.0%. At 400°C, the coal conversion in the petroleum materials range from 28% to 36%. These data indicate and the proton distribution as determined proton nuclear magnetic resonance (1H NMR) substantiate that the petroleum crudes and residua do not contain hydrogen which can be easily

donated to coal. In fact, the majority of the protons in the petroleum materials lie in the alkyl  $\beta$  and  $\gamma$  regions. In these experiments, tetralin, a known hydrogen donor, was the only solvent that produced an increase in oils above that present in the original 2:1 solvent/coal mixture. In the hydrogen deficient atmosphere, donor hydrogen as present in hydroaromatic compounds, appears to be necessary for both coal conversion and the production and maintenance of the oil fraction. Similar results using model hydroaromatic and aliphatic solvents are present in the literature.<sup>8-9</sup>

Compared to the original product distribution, the reaction products from the combined processing lost pentane solubles. A general increase in the asphaltene content of the product liquids was observed as compared with the original charge. In the hydrogen deficient environment, both the coal and the heavy petroleum materials may undergo polymerization forming coke-like material which appears as IOM. In addition, the reacting coal may incorporate a significant portion of the petroleum soluble material into the coal matrix.

Noncatalytic Experiments with a Hydrogen Atmosphere. To eliminate some of the possible retrogressive reactions of the petroleum materials and the coal associated with the inert atmosphere, a hydrogen atmosphere was used. As with the nitrogen atmosphere, tetralin converted the most coal, yielding 71.2%, while the coal-derived material CPDU-200A converted 56.8%. Compared to the nitrogen atmosphere, substantially more coal was converted in the hydrogen atmosphere with the petroleum solvents. The coal conversion ranged from ~43% to 54% depending upon the petroleum material used. The hydrogen atmosphere also either maintained or increased the oil yield as compared to the original charge. Three of the less viscous lighter petroleum materials, Maya Crude, West Texas TLR and Mayan TLR showed a positive increase in oil; whereas, in nitrogen, each of these crudes showed a reduction in oil content when compared to the original solvent. Kuwait resid, West Texas vacuum short and West Texas TLR showed the greatest oil production improvement (> 7%) when a hydrogen rather than a nitrogen atmosphere was used.

Catalytic Liquefaction Using a Hydrogen Atmosphere. The effect of adding a presulfided NiMo/Al<sub>2</sub>O<sub>3</sub> extrudate catalyst on the conversion of coal and on reaction products has also been investigated. The reactions were performed at 400°C and 425°C. For all the solvents used, the addition of presulfided NiMo/Al<sub>2</sub>O<sub>3</sub> increased both oil production and coal conversion. In the compilation of data presented in Table 2, it is apparent that at 400°C and 425°C the presence of the NiMo/Al<sub>2</sub>O<sub>3</sub> hydrogenation catalyst caused a significant improvement in the oil yield. The same improvement is observed in coal conversion. In those cases where the catalytic reactions were performed at both 400°C and 425°C, the twenty-five (25) degree rise in temperature seemed to be a secondary effect on both coal conversion and oil yield with the possible exception of the West Texas vacuum short resid. For West Texas vacuum short resid, coal conversion seemed to be affected by temperature both in catalytic and noncatalytic reactions with hydrogen atmospheres. The addition of a hydrogenation catalyst can significantly improve the oil production and coal conversion in combined processing.

Chemical and Physical Properties of the Petroleum Crudes and Residua. Among the six petroleum materials individual differences are apparent in their ability to convert coal and produce pentane soluble materials. A number of chemical and physical properties of the petroleum materials have been evaluated and are given in Table 1. A typical coal liquid, CPDU-200A, is also shown in Table 1 and has been used as a point of comparison between the coal-derived and petroleum solvents.

From these analyses, general comments can be made concerning the properties of the petroleum solvents. Each petroleum crude and residuum contains large asphaltenic compounds as evidenced by a lack of solubility of ~6 to ~20% of the petroleum material in pentane and that much solubility in benzene. All of the petroleum solvents are hydrogen-rich and high in sulfur as compared to coal-derived liquids.

The typical hydrogen to carbon ratio for coal-derived liquids is 1.0 or less; all of the petroleum crudes and residua used in this study have H/C ratios in the range of 1.45 to 1.65. The ash levels in the petroleum crudes range from 0.012 wt % for West Texas vacuum short resid to 0.082 wt% for Mayan topper long resid. This low ash content is insignificant in this work in terms of the product distribution obtained after coprocessing with coal. All of the petroleum solvents are highly aliphatic, having  $f_a$  values between 0.32 and 0.37. Proton distributions of the petroleum solvents show the protons to be primarily alkyl  $\beta$  and  $\gamma$  protons. Few hydroaromatic protons are present. CPDU-200A, by contrast, is quite aromatic, having a  $f_a$  value of 0.71. A higher percentage of cyclic alpha protons are present in the CPDU-200A than in any of the petroleum materials. The aromatic nature and the presence of some hydroaromatics may account for the CPDU-200A's ability to convert more coal than do the petroleum solvents.

Coal conversion in the petroleum solvents using a hydrogen atmosphere at 400°C can be correlated with the viscosity of the petroleum material and with the Conradson Carbon number. The highly viscous solvents, Kuwait resid and West Texas vacuum short resid, give less coal conversion than do the less viscous petroleum solvents. The petroleum solvents with lower Conradson Carbon numbers promote higher coal conversion. A similar trend is observed with molecular weight. The petroleum solvents with lower molecular weights, Lloydminster reduced crude, West Texas TLR, Maya Crude and Mayan TLR, correlate with increased coal conversion. West Texas TLR which has the lowest Conradson Carbon and the second lowest molecular weight and viscosity gives the highest coal conversion of any of the petroleum solvents during coprocessing. The addition of a catalyst changes the order of the coal conversion among the six petroleum solvents and apparently the relative importance of the solvent's properties. No obvious correlations exist between the abovementioned solvent properties and coal conversion when a catalyst is used.

Parametric Evaluation. The effect of reaction conditions on combined coal and heavy residua processing has been evaluated using the parameters of reaction temperature, initial hydrogen pressure, reaction time and diffusional pathlength of the catalyst. For these studies, Maya Crude was used as the solvent. Three coals were used, Illinois #6, Blacksville, and Clovis Point, with Illinois #6 coal being used for the majority of the experiments. Solvent extraction of Illinois #6 at room temperature showed the coal to be ~90% insoluble at room temperature. When reacted at 425°C in hydrogen in the absence of a solvent, ~35% of Illinois #6 coal was converted, primarily to preasphaltenes. Under the same conditions, ~46% of the Clovis Point was converted with all solubility fractions being present. The upgradability of the Maya Crude was also examined to determine if the asphaltenes present could be upgraded to oil. After thermal reaction the Maya Crude did not change substantively although 2.7% of the product was gas. A 4% increase in oil was observed on catalytic hydrogenation with a further increase in gas production.

Effect of Temperature on the Product Distribution from Illinois #6 and Blacksville Coals. To determine the effect of reaction temperature on the product distributions from coprocessing, the reactions were performed at 375°, 400°, 425°, 450° and 475°C. With increasing temperatures, oil production and higher coal conversion were observed for both coals up to a temperature of 425°C where a maximum in oil yield and a minimum of IOM occurred. For both coals, the greatest coal conversion was observed at 425°C. At higher temperatures, 450° - 475°C, higher gas yields and IOM yields (lower coal conversion) are observed for both coals. Based on these data, a temperature of 425°C was selected for combined processing.

Effect of Initial Hydrogen Pressure on Coprocessing. To determine the sensitivity of combined processing to initial hydrogen pressure, the initial hydrogen pressure was increased from 0 psig to 1500 psig. A powdered Shell 324 NiMo/Al<sub>2</sub>O<sub>3</sub> was added to the reaction mixture. The products distributions shown in Figure 1 demonstrate the need for a hydrogen environment to convert coal and simultaneously to upgrade the petroleum crudes. When no hydrogen is present, only 8.6% coal conversion is

observed. Comparing this conversion to that of thermally reacted coal with no solvent in a hydrogen atmosphere, the hydrogen atmosphere increases coal conversion by more than 20%. In a hydrogen deficient atmosphere, the petroleum solvent may also be undergoing retrogressive reactions forming coke-like materials adding to the IOM. At an initial hydrogen pressure of 250 psig, the pentane solubles produced were higher than that in the original mixture; coal conversion was 52.5%, suggesting that even low levels of hydrogen can be effective in reducing the number of retrogressive reactions when solvent and catalyst are present to aid in the transfer of hydrogen to coal. At 500 psig, the coal conversion again increased significantly to 78.7% while the pentane soluble yields increased to 70.4%. As the hydrogen pressure was increased even further, coal conversion continued to climb yielding 86.9% at 1500 psig. The oil produced also increased at 1500 psig to 78.5%. Above 500 psig, the rate of increase for both coal conversion and pentane soluble yields was lower than between 0 and 500 psig.

Effect of Time and Catalyst Diffusion Pathlength on Product Distributions from the Liquefaction of Illinois #6 Coal. To determine the effect of time on combined processing, three sets of experiments were performed: (1) thermal reaction with no catalyst present, (2) NiMo/Al<sub>2</sub>O<sub>3</sub> pelletized catalysts, and (3) NiMo/Al<sub>2</sub>O<sub>3</sub> powdered catalysts.

A comparison of the ability of Maya Crude to convert coal under these three conditions is given in Figure 2. For all three cases, long reaction time, 90 minutes, increased coal conversion when compared to the shorter time experiments. The use of powdered catalyst increased the amount of coal conversion substantially compared to the thermal and catalyst pellet experiments. This increase occurred for all reaction times. The coal conversion in the thermal and extrudate experiments are very similar and are about 20% less than the powdered catalyst.

From these experiments, it is apparent that the longer residence time the coal has in a hydrogen atmosphere the more coal will be converted. The use of a catalyst increases the availability of the hydrogen to the coal and increases the rate of coal dissolution. The use of a powdered catalyst makes hydrogen more available to the coal by providing contact between the catalyst particles and the dissolving coal matrix. This increased availability is caused by decreasing the diffusional pathlength required for the coal to traverse before coming into contact with an active hydrogenation site.

Hydrogen consumption in the thermal and in both catalytic experiments increased with increasing time. The coprocessing experiments using the powdered catalyst consumed more hydrogen than did either the experiments using pellets or no catalyst. The hydrogen consumption data correlate with the yields of pentane solubles produced under the three conditions. More pentane solubles were produced in the powdered catalyst experiments than in the extrudate experiments which was more than the thermal. The data is presented in Figure 3 which shows the oil production from the three cases as a percentage of the upgradable material present in the reaction, the upgradable material being defined as the maf coal and petroleum asphaltenes present at the beginning of the reaction. The catalyst obviously aids in oil production, with the powdered form yielding significantly greater oil production than the extrudate pellets. These data are a clear indication of the influence of pore diffusional restrictions in limiting the oil yield with extrudate pellets.

Illinois #6 coal was also liquefied in tetralin with a powdered catalyst for 30 minutes. The coal conversion obtained was 92.4% and the oil production was 86.7%. Both the coal conversion and oil production are higher in tetralin than in Maya Crude under equivalent reaction conditions. The values obtained from the combined processing are 81.6% and 76.7%, respectively. Longer reaction times of 90 minutes with Maya Crude produce higher yields of coal conversion and oil, 83.4% and 82.7%, respectively.

The effect of thermal and catalytic combined processing from Clovis Point coal was also evaluated. The product distributions obtained from 30 minutes of reaction are given in Table 4. The product distributions from Clovis Point coal from the three reaction conditions show similar trends to those obtained from Illinois #6 coal. Oil production and coal conversion increased with catalytic treatment, the highest yields being produced from the powdered catalyst. For comparable reaction times, coal conversion from Clovis Point was slightly higher than Illinois #6 for the thermal and pelletized catalyst case. Oil production from Clovis Point coal was consistently 5 to 6% higher than Illinois #6 coal.

#### Summary and Conclusions

Petroleum crudes and residua and coal have been coprocessed at typical liquefaction conditions in atmospheres of nitrogen and hydrogen and in the presence of hydrogen and a catalyst. At 400°C coal conversion in a nitrogen atmosphere was low and at the same level as the thermal coal reaction with no solvent, indicating that no transfer of hydrogen from the petroleum solvents to the coal occurred. Coal conversion increased in the presence of hydrogen; further increases in coal conversion were observed in the presence of catalyst at 400°C and 425°C. The dominant factor of the increased conversion in the majority of the heavy petroleum materials was the presence of the catalyst with the 25° temperature rise being a secondary effect. Oil production from combined processing showed negative or level yields in the N<sub>2</sub> atmosphere, level or slightly positive yields in the H<sub>2</sub> atmosphere and for most petroleum solvents significant increases when a catalyst and hydrogen were both present. As in the case of coal conversion, the catalyst appears to be the dominant factor in the increase with temperature having a secondary effect.

Individual differences among the petroleum solvents are observed in the product distributions obtained from combined processing. Coal conversion in the H<sub>2</sub> atmosphere appears to be correlated with viscosity, molecular weight and Conradson Carbon number of the petroleum crude. These particular solvent characteristics do not seem as important in coal conversion when a catalyst is present.

The parametric evaluation has shown that optimal conditions for combined processing are:

- Reaction Temperature: 425°C
- Hydrogen Pressure: above 500 psig initial hydrogen pressure
- Time: 90 minutes
- Catalyst: powdered hydrogenation catalyst

Coal conversion and oil production from combined catalytic (powdered) processing compare favorably with that from tetralin with a powdered catalyst. Comparison of the final oil yields to the initial charge shows that combined processing yields a net oil increase of 23.3% for 90 minute reaction while tetralin provides a net oil increase of 17.7% for 30 minutes of reaction.

Table 1. Analysis of Liquefaction Solvents

Solvents	Product Distribution (wt.%)		IOM	Ash, wt%	Elemental Analysis				H/C
	Oil	Asphaltenes			Preasphaltenes	C	H	N	
Maya Crude	84.4	15.6		0.058	84.6	11.5	1.21	3.09	1.63
West Texas TLR	93.6	6.4		0.033	86.4	11.0	0.34	2.80	1.51
Mayan TLR	79.5	20.5		0.082	85.3	10.8	0.51	4.19	1.51
Lloydminster Reduced Crude	84.0	16.0		0.039	85.0	10.7	0.34	4.35	1.49
Kuwait Resid	88.96	10.99	0.05	0.031	79.5	10.3	0.19	4.63	1.55
West Texas Vacuum Short Resid	88.7	11.3		0.012	86.1	10.4	0.44	3.33	1.47
CPDU-200A	85.48	12.47	1.16	0.89	89.3	7.3	1.20	0.56	0.97

Solvents	Molecular Weight	$f_a$	$\eta_D$	Viscosity (poise)	Specific Gravity	%API	Conradson Carbon
Maya Crude	577	0.32	1.52		0.920	22.3	10.41
West Texas TLR	545	0.35	1.55	28.2	0.979	13.0	10.34
Mayan TLR	568	0.37	1.56	317	1.000	10.0	15.87
Lloydminster Reduced Crude	481	0.36	1.57	389	1.004	9.44	14.23
Kuwait Resid	961	0.34	1.58	3470	1.014	8.05	17.00
West Texas Vacuum Short Resid	922	0.35	1.58	7075	1.014	8.05	17.33
CPDU-200A		0.71					

Table 2. Effect of Atmosphere and Catalyst on Oil Production and Coal Conversion

Oil, Wt %	West				West			
	Tetralin	Maya Crude	West Texas TLR	Mayan TLR	Lloydminster Reduced Crude	Kuwait Resid	West Texas Vacuum Short	CPDU 200A
Original	67.5	56.9	63.2	53.7	56.7	60.0	59.8	57.7
N <sub>2</sub> , 400°C	70.6	58.7	60.4	53.2	55.7	56.0	54.0	53.4
H <sub>2</sub> , 400°C	71.2	59.9	65.8	56.4	58.8	60.4	58.4	56.3
H <sub>2</sub> + cat, 400°C		69.2			68.1		64.0	
N <sub>2</sub> , 425°C		58.2			51.5			
H <sub>2</sub> , 425°C		62.0	65.1		62.2		58.1	
H <sub>2</sub> + cat, 425°C	83.1	72.3	73.7	66.3	71.5	68.2	66.9	73.8
<u>Average Conversion, %</u>								
N <sub>2</sub> , 400°C	57.2	28.4	30.2	34.9	28.4	30.2	26.7	50.3
H <sub>2</sub> , 400°C	70.6	49.8	53.5	49.3	48.9	45.2	44.5	56.6
H <sub>2</sub> + cat, 400°C		67.3			72.1		52.9	
N <sub>2</sub> , 425°C		28.9			13.2			
H <sub>2</sub> , 425°C		62.5			64.7		58.5	
H <sub>2</sub> + cat, 425°C	81.0	66.2	68.9	62.3	75.2	69.2	65.4	81.6

Table 3. Hydrogen Distributions in Petroleum and Coal-Derived Solvents

Solvents	% Condensed Aromatics		% Uncondensed Aromatics Plus Hydroxyl		% Cyclic $\alpha$	% Alkyl $\alpha$	% Cyclic $\beta$	% Alkyl $\beta$	% $\gamma$
	% Condensed Aromatics	% Uncondensed Aromatics Plus Hydroxyl							
Maya Crude	1.7	2.2	7.2	5.5	16	44	23		
West Texas TLR	3.1	1.2	6.1	4.9	17	46	21		
Mayan TLR	3.6	3.0	7.1	5.9	15	43	22		
Lloydminster Reduced Crude	5.9	2.6	8.5	6.5	18	38	20		
Kuwait	4.6	2.0	7.3	6.6	17	45	18		
West Texas Vacuum Short Resid	7.0	0.0	14	7.0	29	33	9.9		
CPDU-200A	35	13	17	12	8.8	9.7	5.3		

Table 4. Product Distribution of Clovis Point Coal Reacted in Maya Crude Under Thermal and Catalytic Conditions

Product Distribution, wt%	Thermal	Catalyst	
		Pellets	Powder
Gas	5.7	5.7	4.9
Oil	68.4	75.0	81.1
Asphaltenes	9.0	5.5	5.1
Preasphaltenes	5.2	4.9	2.9
IOM	11.7	8.9	6.0
% Coal Conversion	62.3	71.6	80.8

Reaction Conditions: 30 minutes, 1250 psig initial H<sub>2</sub> pressure, agitation 860 cpm, 425°C.

#### References

1. Moschopedis, S. E., Fuel, 590, 1980, 67.
2. Moschopedis, S. E., Hawkins, R. W., Fryer, J. F. and Speight, J. G., Fuel, 59, 1980, 647.
3. Moschopedis, S. E., Hawkins, R. W. and Speight, J. G., ACS Fuel Preprints, 26, (3), 1981, 131.
4. Moschopedis, S. E., Hawkins, R. W. and Speight, J. G., Fuel Processing Technology, Vol. 5, 1982, 213.
5. Mochida, I., Takanabe, A. and Takeshita, K., Fuel, 58, 1979, 17.
6. Mochida, I., Moriguchi, Y., Korai, Y., Fujitsu, H., and Takeshita, K., Fuel, 60, 1981, 746.
7. Mochida, I., Iwamoto, K., Tahara, T., Korai, Y., Fujitsu, A. and Takeshita, K., Fuel, 61, 1982, 603.
8. Neavel, R., Fuel, 1976, 55, 237.
9. Curtis, C. W., Guin, J. A., and Kwon, K. C., AIChE National Meeting, paper 62b, November, 1982.

g o a p i

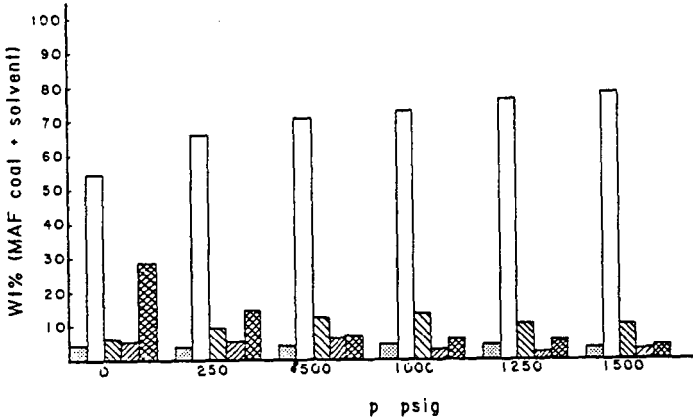


Figure 1. Effect of Initial Hydrogen Pressure on Product Distributions from Combined Processing of Illinois #6 and Maya Crude.

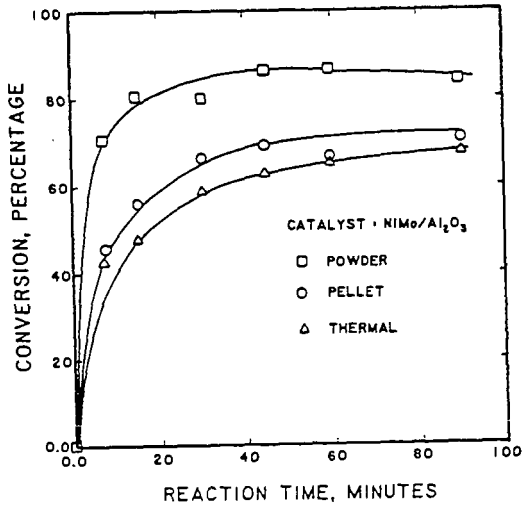


Figure 2. Effect of Time and Catalyst on Coal Conversion from Combined Processing of Illinois #6 Coal and Maya Crude.

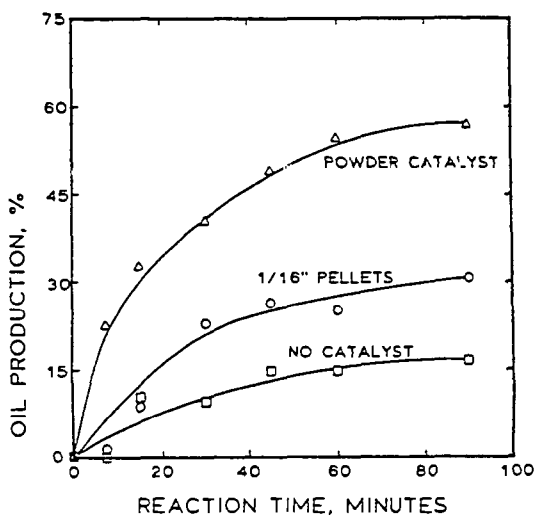


Figure 3. Effect of Time and Catalyst on Oil Production from Combined Processing of Illinois #6 Coal and Maya Crude.

## PYROLYSIS MECHANISMS AND WEATHERING PHENOMENA IN ROCKY MOUNTAIN COALS

Henk L.C. Meuzelaar, William H. McClennen, Candace C. Cady, G. Steven Metcalf,  
Willem Windig, J. Rand Thurgood\* and George R. Hill\*\*

Biomaterials Profiling Center, University of Utah, 391 S. Chipeta Way,  
Suite F, Research Park, Salt Lake City, Utah 84108

\*Utah Power & Light Company, Salt Lake City, Utah 84104

\*\*Chemical Engineering Department, University of Utah, Salt Lake City, Utah 84108

### INTRODUCTION

During the past decade coal scientists and technologists have become increasingly aware of the potentially dramatic effects of oxidation ("weathering") on the structure and reactivity of coals. Presently known effects range from autoignition in mines [1] and piles [2], changes in electrostatic charge, slurry pH and flotability [3] or loss of caking properties [4-7] and calorific value [3,4] to decreased tar [8,9] and volatile matter yields, increased char yields [9,10] and altered char properties [3,5,6]. An excellent overview of coal weathering effects can be found in a recent paper by Cox and Nelson [11].

Because of a lack of generally accepted and standardized procedures for determining the degree of weathering (the "weathering index") of a given coal sample, most data on structure and reactivity reported in the literature thus far were obtained on coal samples of uncertain weathering status and should therefore be interpreted with great caution.

Unfortunately, this situation is compounded by the difficulty of obtaining "non-weathered" coal samples for structure and reactivity tests since even reference samples available from coal sample banks have sometimes been found to exhibit signs of weathering. In the near future a new collection of standard coal samples, the Premium Coal Sample Program currently underway at Argonne National Laboratory under the most stringent anaerobic collection, preparation and storage conditions [12], may help solve the availability problem. In the coal weathering experiments reported here high volatile B bituminous coal samples obtained directly from freshly exposed seam facies in the Wasatch Plateau field (Hiawatha and Blind Canyon seams, Emery County, Utah) were used.

The present study was prompted by the discovery of FSI values as high as 4.0 in coals obtained directly from fresh mine cuts in the Hiawatha and Blind Canyon seams [4]. Until then, coals from these seams were generally considered to be noncaking. Since FSI values  $> 2.0$  could interfere with pyrolytic conversion schemes under consideration by Utah Power and Light Company [13], a systematic study of the influence of weathering on the reactivity and structure of selected Wasatch Plateau coals was undertaken.

### EXPERIMENTAL

Several hundred pounds of samples were obtained from the top, middle and bottom of freshly exposed cross sections of the Hiawatha and Blind Canyon seams and immersed in water until being crushed and milled to  $< 60$  mesh in a nitrogen atmosphere. All sample storage took place under nitrogen in hermetically closed glass bottles at  $-20^{\circ}\text{C}$  in the dark. In the laboratory weathering experiments, 10-15 g aliquots of  $< 60$  mesh coal were exposed to different temperatures and atmospheric conditions ( $\text{N}_2$  or air; dry or  $\text{H}_2\text{O}$  saturated) for periods up to several weeks or months using a specially constructed bench scale weathering system [4].

FSI determinations were performed according to ASTM Standard D-720-67, whereas standard ASTM proximate analysis, calorific value and total sulfur determinations were carried out by Standard Laboratories (Huntington, Utah). TG/DTG analyses were performed with a Mettler I thermal analyzer under the following conditions: (initial pyrolysis run) sample weight approx. 10 mg, nitrogen flow 100 ml/min, heating rate 15°C/min, end temperature 790°C, (subsequent char combustion run; after cooling down) air flow 100 ml/min, heating rate 15°C/min, end temperature 990°C.

Curie-point pyrolysis mass spectrometry was performed with an Extranuclear 5000-1 instrument under the following conditions: sample weight 20 µg (deposited from a fine suspension in MeOH), heating rate approx. 100°C/s, end temperature 610°C, total heating time 10 s, electron energy 12 eV, mass range scanned m/z 20-260, total number of spectra summed 150, total scanning time 30 s. Computerized data analysis involved normalization of signal intensities by means of the NORMA program [14] followed by factor analysis, discriminant analysis and canonical variate analysis using the SPSS program package [15].

## RESULTS AND DISCUSSION

The FSI was found to be a highly sensitive indicator of the weathering status of these coals with a slight, but measurable drop in FSI value occurring overnight upon exposure of fresh coals to air at room temperature. Typical FSI weathering profiles are shown in Figure 1. Since coal weathering is often accompanied by complex weight changes due to the interplay of fluctuations in moisture content and oxidative phenomena, a series of weathering experiments was carried out while carefully monitoring changes in sample weight, as shown in Figure 2. Weight corrected weathering trends of several conventional parameters are illustrated in Figure 3a and Table 1 showing how misleading results are obtained if the original weight of the non-weathered sample is unknown (as is usually the case). Note that the weight corrected change in calorific value is -1.1% after 96 hours at 80°C in air and -2.1% at 100°C in air.

Much more informative about changes in reactivity and structure are the Thermogravimetry (TG) and Derivative Thermogravimetry (DTG) data in Figures 4 and 5 and, in particular, the Pyrolysis Mass Spectrometry (Py-MS) data in Figures 6, 7, 8 and 9. The TG/DTG pyrolysis data in Figures 4a and 5a would seem to support a weathering mechanism dominated by the formation of crosslinks between coal molecules, thereby causing a widening of the temperature range of the pyrolysis process and a decrease in the maximum pyrolysis rate accompanied by increased char yields while having little or no influence the maximum rate temperature (~450°C). The results of the char combustion runs in Figures 4b and 5b indicate a similar kinetic trend (decreased reaction rate and increased temperature range) but are less definitive due to a lower level of reproducibility than in the pyrolysis runs.

Inspection of the pyrolysis mass spectra in Figure 6 shows the structural effects of weathering to be dominated by a decreased yield of phenolic and naphthalenic moieties and a relative increase in the yield of aliphatic carboxylic and carbonylic moieties, as further illustrated by the scatter plots of selected peak intensities in Figure 7. These findings are in excellent agreement with current views on chemical effects of coal weathering, according to which the process is characterized by the formation of ether bridges between aromatic nuclei with concurrent reduction in free phenolic hydroxyl groups [16], and by the oxidation of aliphatic moieties to carbonylic and carboxylic functional groups [17]. A more detailed picture of the complex changes in the pyrolysis mass spectra can be obtained by means of multivariate analysis techniques such as discriminant analysis, as illustrated in Figure 8. The application of these techniques to the evaluation of pyrolysis mass spectra of coal has been described elsewhere [14,18,19]. The discriminant analysis results in Figure 8 show that: (a) the first discriminant function exhibits no detectable changes in the coal spectra upon "weathering" at 80°C in a nitrogen atmosphere, (b)

weathering effects at 80°C and 100°C in air show strong quantitative differences, (c) several other series of aromatic, hydroaromatic and hydroxyaromatic compounds appear to decrease besides phenols and naphthalenes, and (d) the changes in aliphatic moieties are much more complex than the simple formation of carbonylic and carboxylic groups. Examination of the second discriminant function (not shown) confirmed the absence of detectable changes at 80°C in N<sub>2</sub> but revealed the presence of slight but significant qualitative differences between the 80°C and 100°C weathering trends, apparently reflecting transient chemical phenomena (peroxide formation?) during the weathering process.

Although, at first sight, the "classical" coal weathering concept of crosslinking through ether bridge formation between macromolecular chains appears to fit our observations quite well, modern views of vitrinite as a binary system consisting of a "mobile" phase and a macromolecular "network" phase necessitate a rethinking of the crosslinking concept. The binary phase model, recently summarized by Given [20], assumes that up to 50% or so of the bulk of the coal sample consists of relatively small, mobile molecules trapped in cages formed by a macromolecular network which makes up the remainder of the bulk. Direct evidence for the presence of a trapped mobile phase can be obtained by Time-resolved Py-MS, as shown in Figure 9. Approximately 50% of the C<sub>2</sub>-alkylnaphthalene signal in Figure 9 is recorded well below typical pyrolysis temperatures for covalent bonds but far above the expected vacuum distillation point for these compounds. A crude attempt to visualize the proposed binary phase system is presented in Figure 10, demonstrating that, in principle, three possibilities for intermolecular bond formation exist in such a system: (1) "crosslinking" between network chains, (2) "condensation" between mobile phase constituents, and (3) "grafting" of mobile phase constituents onto the network chains.

To obtain a better insight into the behavior of the two phases, fresh and artificially weathered (212 hrs at 100°C in air) Hiawatha coal samples were submitted to vacuum distillation (30 hrs at 180°C and 10<sup>-3</sup> Torr), pyridine extraction (24 hrs in Soxhlet extractor), short contact time (SCT) pyrolysis in a tubing bomb reactor (2.5 g coal in 5.0 g benzene, heating rate 20°C/s, end temperature 420°C, total heating time 40 s, H<sub>2</sub> pressure 1,000 psi initial to 1,700 psi final) and direct Curie-point Py-MS (1.5 X 10<sup>-5</sup> g coal in vacuo, heating rate 100°C/s, end temperature 610°C, total heating time 10 s). Subsequently, the distillates, extracts or pyrolyzates, as well as the residues were analyzed by Py-MS. Preliminary results are shown in Table II and illustrate the dramatic effect of weathering on vacuum distillation yields, pyridine extraction yields and SCT tubing bomb reactor (TBR) pyrolysis yields. The yield of the small vacuum distillate fraction (4%, dominated by alkylnaphthalenes; see Figure 11a), shows a fourfold decrease upon weathering. The much larger pyridine-extractable fraction (22%, also dominated by alkylnaphthalenes but containing significant contributions from other aromatic moieties; see Figure 11b) decreases by a factor of five to six after weathering.

Hydroxyaromatics (e.g., phenols, dihydroxybenzenes), which are among the most abundant homologous ion series in pyrolysis mass spectra of fresh whole coals (see Figure 11d) are nearly absent in the vacuum distillate (Figure 11a) and relatively low in the pyridine extract (Figure 11b) but make a more prominent appearance among the SCT-TBR products shown in Figure 11c. Probably these hydroxyaromatics are partially produced through pyrolytic bond scissions and thus may represent the network phase. Additional support for this contention is provided by the much smaller reduction factor (2X) for the SCT-TBR yields from weathered coal.

A speculative interpretation of these findings might envisage a mobile phase representing 20-30% of the bulk of the fresh Hiawatha coal and undergoing a 4-6 fold reduction under the above weathering conditions. Presumably, this reduction is due to the formation of strong (diarylether?) bonds with hydroxyaromatic moieties in the network phase ("grafting"; see Figure 10). On this view, SCT pyrolysis results in

partial degradation of the network into hydroxyaromatic compounds and other small, mobile molecules. However, the pyrolysis conditions used appear to leave most of the new bonds formed in the weathering process intact, thus resulting in a marked decrease in overall pyrolysis yields from weathered coals.

Visual comparison of the four MS patterns in Figure 11 reveals an obvious trend towards increasing complexity from the vacuum distillate (Figure 11a) to the Curie-point pyrolyzate (Figure 11d). For the first three fractions this trend corresponds directly with increasing yields (from 4% for the vacuum distillate to 38% for the TBR pyrolyzate) and, if extrapolated, would indicate a yield of between 40-50% for the Curie-point pyrolyzate, which is in good agreement with previous estimates for hvb Utah coals [18].

At the same time, these observations highlight the fact that under SCT pyrolysis conditions some 50% of the (m.a.f.) coal forms a char. This char, which is difficult to analyze by most techniques currently available, might incorporate as much as 2/3 of the network phase. This leads to the question whether the pyrolysis products obtained from the network phase are representative for the overall chemical structure of the network. In his comprehensive discussion of the binary phase nature of coal, Given [20] concludes that in spite of all available data from sophisticated analytical methods, including FTIR and <sup>13</sup>C NMR, the chemical nature of the network phase remains pretty much a mystery.

If the binary phase concept is valid indeed, much effort will have to be devoted to the elucidation of key structural features of the macromolecular network if a more comprehensive picture of the effects of weathering on the structure and reactivity of coals is to be obtained within the foreseeable future.

#### REFERENCES

1. Saranchuk, V.I., Khimiya Tverdogo Topliva, Solid Fuel Chemistry, 11, 63 (1977).
2. Bouwman, R. and Freriks, I.L.C., Fuel, 59, 315 (1980).
3. Gray, R.J., Rhoades, A.H. and King, D.T., AIME, Transactions, 260, 334 (1976).
4. Hill, G.R., Meuzelaar, H.L.C., "Free Swelling Index of Utah High Volatile Bituminous Coals", Report to UP&L Co., contract R&D 1003-83, Sept. 1982-Aug. 1983.
5. Crelling, J.C., Schrader, R.H. and Benedict, L.G., Fuel, 58, 542 (1979).
6. Habermehl, D., Orywal, F. and Byer, H.-D., "Chemistry of Coal Utilization, 2nd Supp. Vol., M.A. Elliot, Ed., Wiley-Interscience, New York, 1981.
7. Wachowska, H.M., Nandi, B.N. and Montgomery, D.S., Fuel, 53, 212 (1974).
8. Wachowska, H., Pawlak, W., Fuel, 56, 422 (1977).
9. Furmisky, E., MacPhee, J.A., Vancia, L., Ciavaglia, L.A., Nandi, B.N., Fuel, 62, 295 (1983).
10. Gromicko, F.N., Sarott, L., Gasior, S., Strakey, J., ACS, Div. Fuel Chem. Preprints, 23, 121 (1978).
11. Cox, J.L. and Nelson, C.R., ACS, Div. Fuel Chem. Preprints, 29, 102 (1984).
12. Premium Coal Sample Program Information obtained by Dr. K. Vorres, Argonne.
13. Thurgood, J.R., Presented Synfuels 3rd Worldwide Symp. Wash. D.C., Nov. 1983.
14. Harper, A.M., Meuzelaar, H.L.C., Metcalf, G.S., Pope, D.L., in "Analytical Pyrolysis Techniques & Applications", K.J. Voorhees, ed., Butterworth, in press.
15. Nie, N.H., Hull, C.H., Jenkins, J.G., Steinbrenner, K. & Bent, D.H. (eds.) Statistical Package for the Social Sciences (SPSS), McGraw Hill, NY, 1975.
16. R.C. Neavel, in "Coal Science", Gorbaty, Larsen, & Wender (eds) Academic Press, 1982.
17. Painter, P.C., Snyder, R.W., Pearson, D.R. and Kwong, J., Fuel, 59, 282 (1980).
18. Meuzelaar, H.L.C., Harper, A.M., Hill, G.H., Fuel, in press (1984).
19. Schenck, P.A., de Leeuw, J.W., Viets, T.C., Haverkamp, J., in Petroleum Geochemistry and Exploration of Europe, Brooks, J. (ed.), Blackwell, 267.
20. Given, P.H., in "Coal Science", M. Gorbaty, Larsen, J.L., Wender, I., Academic Press, NY 1984 (in press).

CREDIT

The work reported here was sponsored by research contracts from Utah Power and Light Company and the U.S. Department of Energy (contract #DE FG22-82-PC50970).

TABLE I  
EFFECT OF WEATHERING ON CALORIFIC VALUE

Calorific Value (BTU)	Fresh	80°C in N <sub>2</sub> 120 hours	Δ* (%)	80°C in air 96 hours	Δ* (%)	100°C in air 96 hours	Δ* (%)
- as received	12028	12556	+4.4	12299	+2.3	12063	+0.3
- dry	12457	12575	+0.9	12318	-1.1	12078	-3.0
- weight corrected	12028	12003	-0.2	11893	-1.1	11773	-2.1

\* difference with corresponding "fresh" value.

TABLE II  
WEATHERING EFFECTS ON HIAWATHA COAL PROCESS YIELDS

Process	% Yield	
	Fresh Coal	Weathered Coal
Vacuum Distillation	4	1*
Pyridine Extraction	22	4
SCT-TBR Pyrolysis	38	17

\* Value from a single experiment; all other values averaged from two or more experiments.

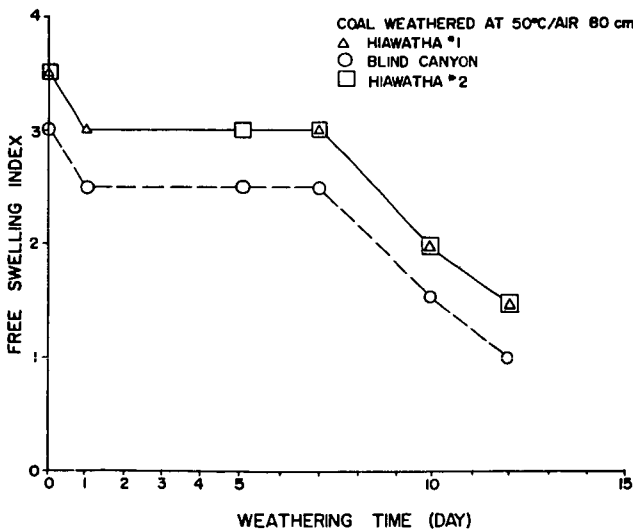


Figure 1. Effect of weathering at 50°C in air on FSI of coal samples from one Blind Canyon and two Hiawatha seam mines.

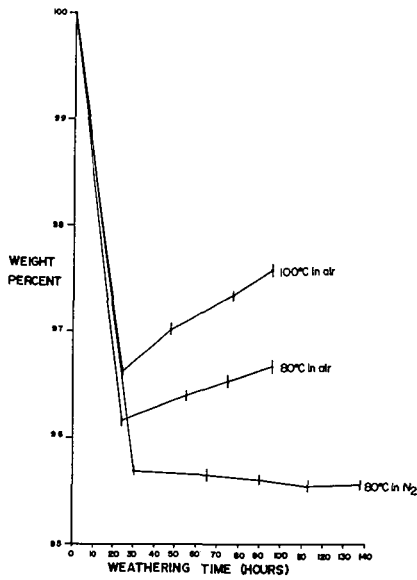


Figure 2. Effect of weathering on weight of Hiawatha seam coal. Note usefulness of control samples in N<sub>2</sub> for distinguishing effects of moisture loss (-4.4%) from effects of oxidative weight gain. Error bars represent range of values for three independently weathered aliquots.

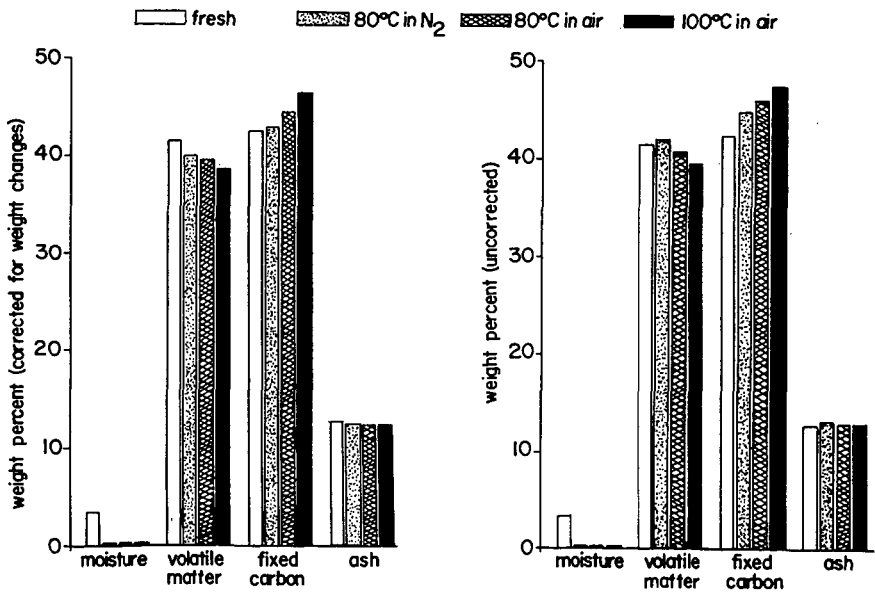
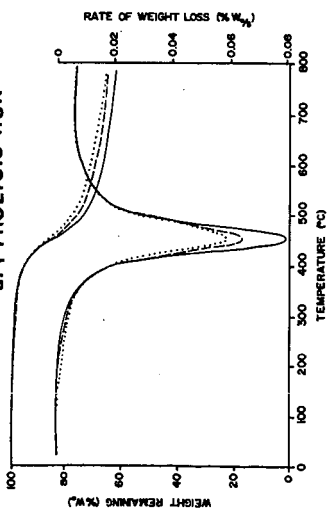


Figure 3. Effect of weathering on proximate analysis of Hiawatha coal.

**a. PYROLYSIS RUN**



**b. CHAR COMBUSTION RUN**

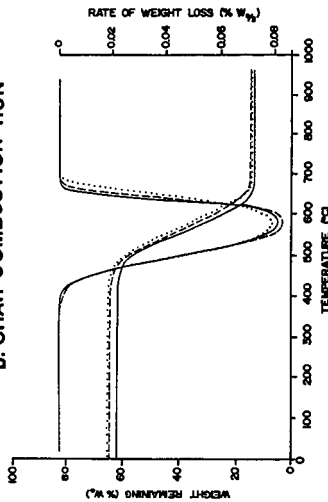
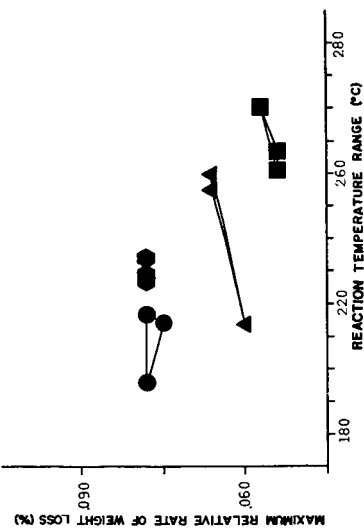


Figure 4a and b. Effects of weathering on TG/DTG profiles of Hiawatha coal. Each curve averaged from three replicate runs.  $W_0$ =original sample weight. — fresh coal; --- weathered at 80°C in air (96 hours); .... weathered at 100°C in air (96 hours).

**a. PYROLYSIS RUN**



**b. CHAR COMBUSTION RUN**

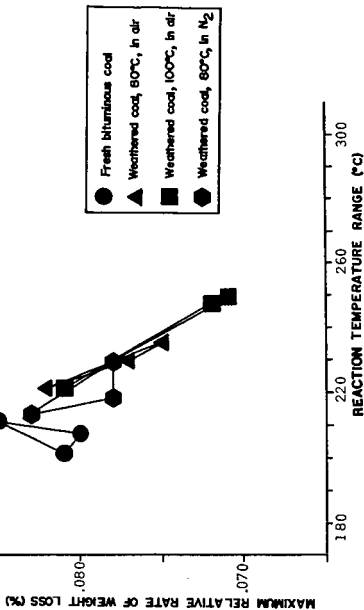


Figure 5a and b. Effects of weathering on selected TG/DTG parameters. The "Reaction Temperature Range" is defined as the temperature range over which the (pyrolysis or combustion) reaction rate is  $\geq 3\%$  of the maximum rate (compare with Figure 4). Data points on replicate weathering experiments connected by solid lines.

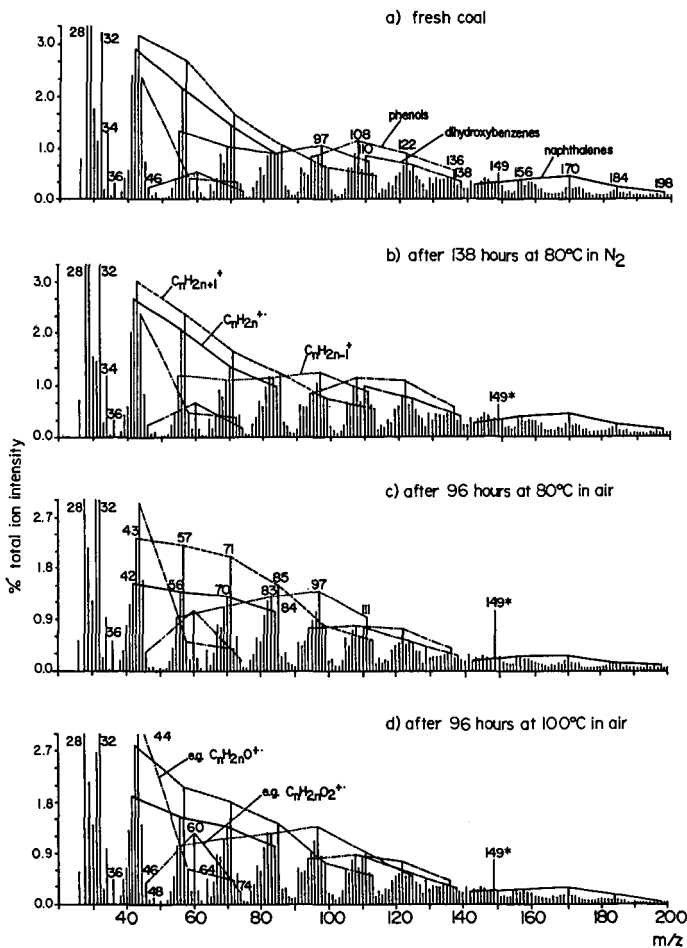


Figure 6. Curie-point pyrolysis mass spectra of fresh and weathered Hiawatha coal samples. Note high degree of similarity between spectra a) (fresh coal) and b) (80°C in N<sub>2</sub>) and obvious changes in spectra c) (80°C in air) and d) (100°C in air). Overall weathering effects appear to be: decreased aromatic series; increased carbonylic (C<sub>n</sub>H<sub>2n</sub>O) and carboxylic (C<sub>n</sub>H<sub>2n</sub>O<sub>2</sub>) series; decreased H<sub>2</sub>S peak (m/z 34); increased CO<sub>2</sub> (m/z 44) and SO<sub>2</sub> (m/z 64) peaks; increased MeOH solvent retention (m/z 23); altered distribution of aliphatic hydrocarbon series. The phthalate fragment ion peak at m/z 149 may be due to contamination.

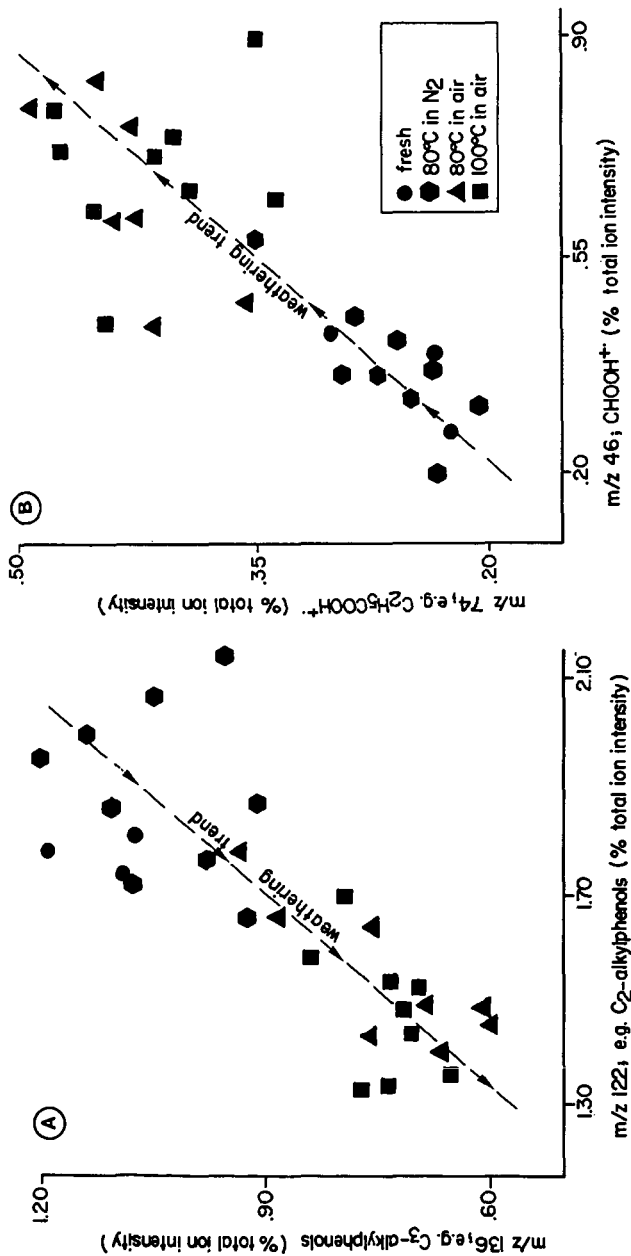


Figure 7 a and b. Scatter plots of selected ion intensities from the pyrolysis MS data set (compare with Figure 6) showing the effects of weathering on alkylphenol signals (strong decrease; see Figure 7a) and on short chain carboxylic acid signals (marked increase, see Figure 7b).

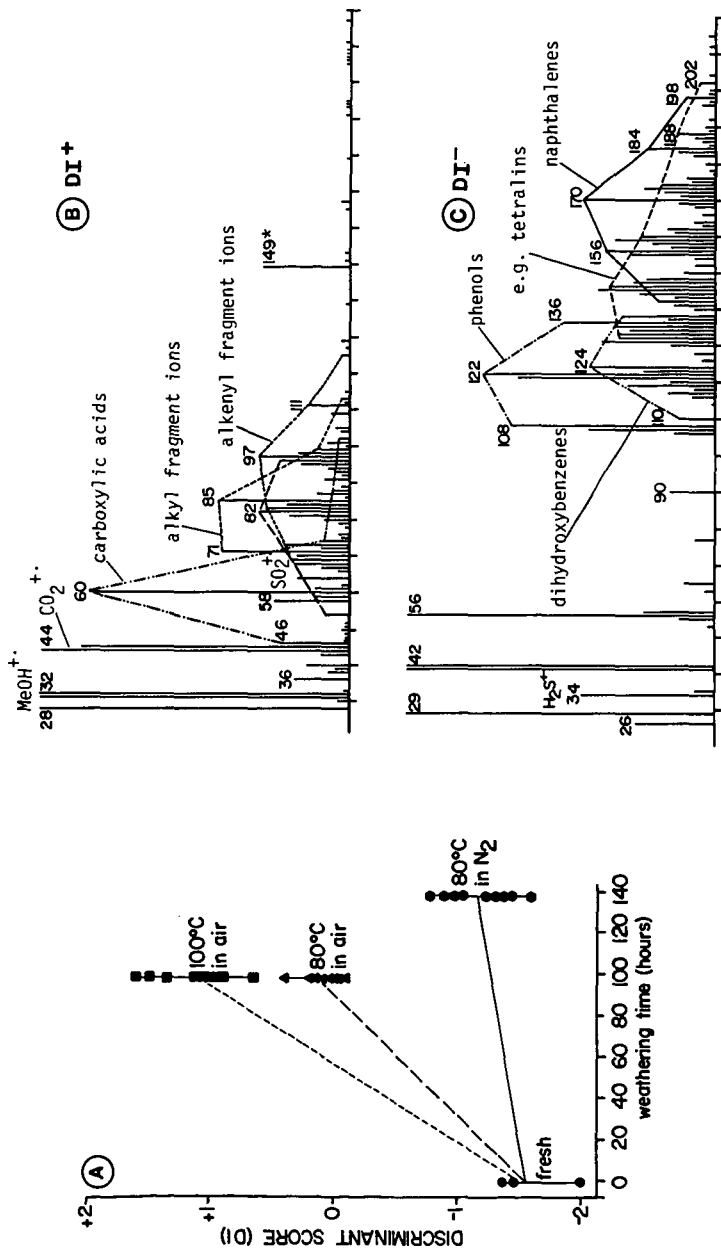


Figure 8. Discriminant score plot and associated "discriminant spectra" obtained on pyrolysis mass spectra of fresh and weathered Hiawatha coal samples (see Figure 6). Air and N<sub>2</sub> exposures were carried out with three different aliquots analyzed in triplicate, resulting in 27 spectra representing 3 categories (80°C in N<sub>2</sub>, 80°C in air, 100°C in air). The triplicate spectra of the fresh coal sample were treated as "unknowns" in the discriminant analysis procedure. The two spectra correspond to the positive (DI<sup>+</sup>) and negative (DI<sup>-</sup>) components of the discriminant function.

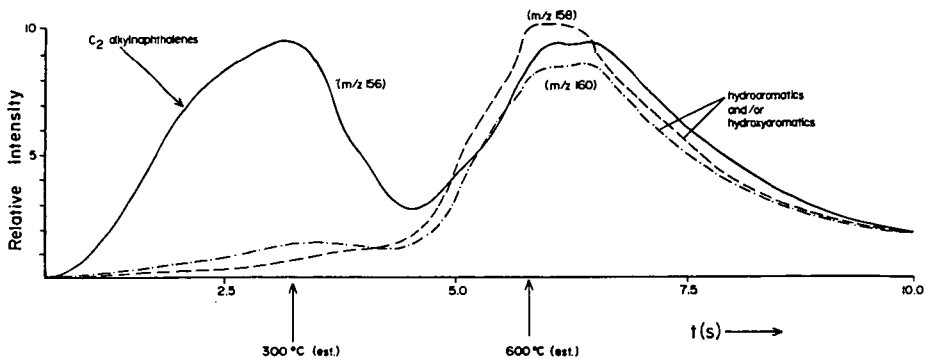


Figure 9. Time-resolved recording of the mass peaks at  $m/z$  156 (mainly  $C_2$ -alkylnaphthalenes),  $m/z$  158 (e.g., methyl naphthol and/or  $C_2$ -alkyl dihydronaphthalenes) and  $m/z$  160 (e.g.,  $C_2$ -alkyl tetralins) during Curie-point pyrolysis of a 20  $\mu\text{g}$  sample from a hvb Wasatch Plateau coal. Note bimodal character of the signal at  $m/z$  156.



Figure 10. Highly schematized representation of all three possible types of weathering-induced bridge formations in a binary phase (mobile phase/network phase) coal model.

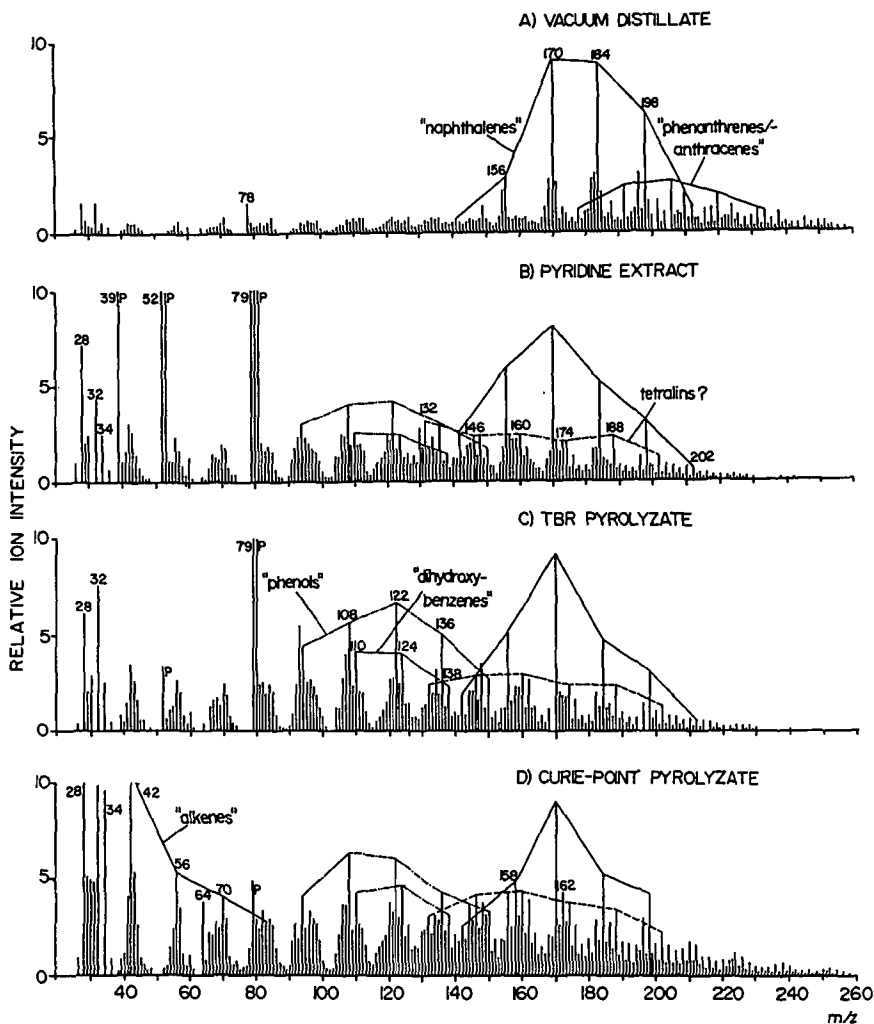


Figure 11. Curie-point desorption/pyrolysis mass spectra of tar fractions from a nonweathered ("fresh") Hiawatha coal obtained by different techniques. Compare with Table I. Note increasing complexity from a to d (exaggerated in d by the presence of gaseous, low molecular weight products, e.g., alkenes, lost during collection of a-c). Peaks labeled "P" represent pyridine residues and/or background signals.

## THE ACTIVITY OF Cu-ZnO-Al<sub>2</sub>O<sub>3</sub> METHANOL SYNTHESIS CATALYSTS

G C Chinchen, P J Denny, D G Parker, G D Short,  
M S Spencer, K C Waugh† and D A Whan

Imperial Chemical Industries PLC, Agricultural Division,  
PO Box No 1, Billingham. Cleveland, England

† ICI New Science Group, Runcorn Heath, Runcorn,  
Cheshire, England

Methanol is made (1) with greater than 99% selectivity when a high pressure gas mixture of CO, CO<sub>2</sub> and H<sub>2</sub> is passed over a catalyst containing Cu, ZnO and Al<sub>2</sub>O<sub>3</sub> at between 220°C and 300°C. Other than that the reaction is exothermic there seem to be few further facts about which complete agreement exists (2, 3). With increasing emphasis being placed worldwide on methanol synthesis processes because of the possible role which methanol may play in the future either as a feedstock or a fuel, there is now a considerable interest in the chemistry of the synthesis reaction. We have sought for many years to gain an understanding of the mechanism of methanol synthesis on Cu-ZnO-Al<sub>2</sub>O<sub>3</sub> catalysts for the purely pragmatic reason that we hope thereby to discover ways of improving, still further, the already impressive performance characteristics of these catalysts.

Our approach has been to apply a wide range of techniques, particular emphasis being placed, where possible, on the use of practical catalysts under industrial working conditions, with the aim of answering the following questions:

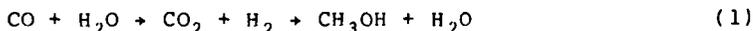
- (i) Is methanol synthesised from CO or CO<sub>2</sub>?
- (ii) What is the state of the copper in a working catalyst?
- (iii) What roles are played by the ZnO and Al<sub>2</sub>O<sub>3</sub> components in the commercial catalyst?
- (iv) What is the mechanism and which reaction step is rate determining?
- (v) What are the active sites for methanol synthesis on a Cu/ZnO/Al<sub>2</sub>O<sub>3</sub> catalyst?

## MEASUREMENT OF CATALYST ACTIVITY

Activity is determined under standard conditions of 250°C, 50 atms, SV 40,000 hrs<sup>-1</sup>, gas composition 10% CO, 3% CO<sub>2</sub>, 67% H<sub>2</sub>, 20% N<sub>2</sub> in standardised pseudoisothermal reactors operating from a single large gas battery with a common purification system. Each catalyst sample is reduced under standard conditions (5% H<sub>2</sub> in N<sub>2</sub> at 1 atm for 15 hrs) and exposed to reaction gas for pre-set periods of time. To a first approximation, activity is proportional to methanol concentration in the outlet gases - an assumption reasonably defensible provided catalyst activity does not vary too widely between samples, and as long as equilibrium is not closely approached. The reproducibility of activity measurements is shown by the exit concentration of methanol (measured to 99% confidence limits) from 23 replicate runs with a standard industrial catalyst. An arbitrary activity of unity was assigned to this catalyst.

## THE ROLE OF CARBON DIOXIDE

In 1975 Kagan et al<sup>4</sup> reported work with labelled carbon oxides which showed that methanol synthesis proceeds through carbon dioxide rather than carbon monoxide eg



This work has been repeated and confirmed by us. With <sup>14</sup>CO<sub>2</sub> as a component, gas containing equal moles of CO and CO<sub>2</sub>, has been reacted over the standard Cu-ZnO-Al<sub>2</sub>O<sub>3</sub> catalyst under the standard conditions as described above. Space velocity was varied between 10,000 and 240,000 hrs<sup>-1</sup> and the exit gases analysed for the separated components and their corresponding radioactivities measured. Results are shown in Figure 1 and reveal clearly that synthesis proceeds via carbon dioxide. 'Scrambling' of radioactivity via the shift reaction:



is negligible at high space velocities and indicates that under methanol synthesis conditions the reverse water gas shift reaction (ie left to right above) is slower than the methanol synthesis reaction. This coupled with the fact that methanol radioactivity is always higher than that of the CO<sub>2</sub>, suggests there may be no intermediate common to the water gas shift and synthesis reaction.

## THE STATE OF COPPER IN A WORKING CATALYST

Accurate measurement of the copper surface area of reduced Cu-ZnO-Al<sub>2</sub>O<sub>3</sub> catalysts by the use of the reaction between nitrous oxide and surface copper atoms is now routine and reproducible.

The method has been described by previous authors (5, 6) and in its most convenient form the evolution of nitrogen following a pulse of nitrous oxide is measured. With this technique a number of Cu-ZnO-Al<sub>2</sub>O<sub>3</sub> catalysts of different synthesis activity and covering a range of copper particle sizes has been examined. The results shown in Figure 2 illustrate a linear dependence of synthesis activity on total copper surface area.

In this work we have adhered to the standard reduction procedure because the resulting surface is representative of the initial state of the real catalyst surface in industrial use. Reduction, however with either CO or pure H<sub>2</sub>, results in a 25% increase in copper surface area showing that some copper still remains oxidised after standard reduction treatment.

The available metal surface area associated with a working catalyst surface can be measured in a variation of the technique by sweeping the working system clean with inert gas and then switching in a pulse of nitrous oxide. The efficacy of this treatment can be measured by fully re-reducing the oxidised surface and redetermining the total surface area to ensure that no irreversible surface changes have occurred. Results shown in Table 1 reveal that about 30% of the initial copper surface of a typical industrial catalyst is unavailable for reaction with nitrous oxide under working conditions, ie is probably oxidised. The proportion of oxidised sites on the working surface will almost certainly be a function of the ratios of carbon dioxide to carbon monoxide and of steam to hydrogen as well as temperature. The catalyst surface is therefore in a dynamic state and it may be anticipated that the nature of the surface will vary in a fixed bed reactor from top to bottom, being a function of the ambient gas composition. This emphasises the uncertainties inherent in extrapolating from experimental results obtained under conditions differing significantly from those used practically.

The oxidised surface of the copper crystallites probably consist partly of O<sub>(ads)</sub> and OH<sub>(ads)</sub>. The interchange of these species via hydrogen and water is well established (7-9) and likely to occur under methanol synthesis conditions.

## THE ROLE OF SUPPORT OXIDES

The establishment of a correlation between copper surface area and methanol synthesis activity does not rule out a role for the supporting oxides in the detailed mechanism of synthesis. For example, some essential, but not rate-determining, steps in the reaction mechanism may occur on the support. Alternatively, if the surface/adsorbate complex involved in the rate determining step were a copper species, the presence of which was determined by juxtaposition with zinc oxide (zinc-copper contiguity) then the copper surface area correlation given above would still be obtained.

However, certain possible roles can be ruled out, for example, rate determining adsorption of any species onto a zinc or aluminium site.

One way in which evidence can be brought to bear on the role of zinc or aluminium oxides is to prepare high area catalysts in which one or the other oxide is omitted and to measure the activity/unit copper area compared with a standard copper-zinc-alumina catalyst. This has been done for a series of binary compositions containing copper allied respectively with the oxides of aluminium, manganese and magnesium. Results are shown in Figure 3 and compared with the standard Cu-ZnO-Al<sub>2</sub>O<sub>3</sub> correlation. To a first approximation they reveal, surprisingly, no unique role for either zinc oxide or alumina in determining methanol synthesis activity. The copper surface areas of these catalysts under synthesis conditions are given in Table 1. As with the Cu-ZnO-Al<sub>2</sub>O<sub>3</sub> catalysts, re-reduction gave an increase in copper area in all but one sample, but the proportion of copper surface covered by oxide was always much smaller. The high level of surface oxidation in copper/zinc catalysts may be a consequence of surface brass formation.

The area measurements therefore strongly suggest that only copper metal/copper oxide and probably only the copper metal surface is implicated in the rate determining step of synthesis and any oxide with appropriate basicity is substantially equally effective in promoting copper surface area and corresponding synthesis activity. Considerations of catalyst stability are, of course, not pertinent at this point.

## MECHANISM OF METHANOL SYNTHESIS

The combination of temperature programmed desorption (TPD) and temperature programmed reaction spectroscopy (TPRS) has been used to examine the mechanism via adsorption, desorption and decomposition of reaction intermediates. These techniques have shown that on Cu/ZnO/Al<sub>2</sub>O<sub>3</sub> catalysts, the observed intermediate on the surface of the Cu and ZnO components of the catalyst is the formate species. Methanol adsorption (Figure 4) at room temperature on to a catalyst in which the surface copper is about 25% oxidised (see above) was characterised by two main peaks in the desorption spectrum: (i) by the coincident desorption of H<sub>2</sub> and CO<sub>2</sub> at a peak maximum temperature of 440K - a fingerprint of the existence of a formate species adsorbed on the copper component (10) and (ii) by the coincident desorption of H<sub>2</sub> and CO at 580K - characteristic of a formate species adsorbed on zinc oxide (11, 12).

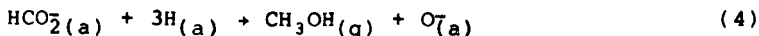
The same two formate species are observed after the adsorption of formaldehyde on this partially oxidised catalyst, in addition to which methanol itself is desorbed at 360 K. This latter is characteristic of desorption of methanol from copper 110 (13), suggesting that it has in fact been formed on the copper component of the catalyst in preference to the zinc oxide component.

A pointer to the rate determining step on the copper component of the catalyst and an indication of the role of the support in the mechanism is to be found in microreactor experiments (1 at) on a Cu/Al<sub>2</sub>O<sub>3</sub> catalyst. Following CH<sub>3</sub>OH synthesis, TPRS showed that the formate species existed on the surface of the copper under steady state methanol synthesis conditions (CO<sub>2</sub>/H<sub>2</sub> feed, 220°C); the same formate species was observed after dosing the catalyst continuously with the same feed (CO<sub>2</sub>/H<sub>2</sub>), but at 100°C, when no detectable reaction occurred, ie neither methanol synthesis nor reverse shift. The rate determining step in the conversion of CO<sub>2</sub> and H<sub>2</sub> to methanol on the copper component of the catalyst occurs therefore after formation of the surface formate species - probably the hydrogenolysis of the adsorbed formate. TPD experiments on the Cu/Al<sub>2</sub>O<sub>3</sub> catalyst and on Al<sub>2</sub>O<sub>3</sub> alone showed the CO<sub>2</sub> to be adsorbed on the alumina itself, suggesting that a role of the basic support (both Al<sub>2</sub>O<sub>3</sub> and ZnO) is the adsorption of the CO<sub>2</sub>. This could then react at the support/copper interface with hydrogen atoms adsorbed on the copper, forming a formate species on the copper surface, the rate determining step probably being the hydrogenolysis of this adsorbed formate.

Alternatively, at working pressures (50-100 at), CO<sub>2</sub> may adsorb on the partially-oxidised copper surface and then react in the same way. Such adsorption of CO<sub>2</sub> has been reported by Stone and Tilley (14) for a copper surface, partially oxidised by molecular oxygen. It is clear from these results and those described above, that the adsorption of CO<sub>2</sub> is not rate determining.

The nature of the adsorbed CO<sub>2</sub> has been suggested in ab initio, self consistent field molecular orbital calculations (15) which showed that unlike other possible molecular interactions no energy barrier existed for the reaction of hydrogen atoms with CO<sub>2</sub><sup>-</sup>.

The overall methanol synthesis mechanism from CO<sub>2</sub> and hydrogen can therefore be written as:



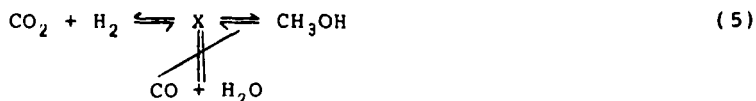
where the subscript a and g relate to adsorbed and gas phase species respectively. The negative charge on the adsorbed CO<sub>2</sub> and formate species may be less than unity.

The mechanism does not specify which of the three hydrogenation steps represented by reaction 4 is rate determining, but it seems likely that it is the step which involves carbon-oxygen bond breakage, ie hydrogenolysis.

However, as reaction 4 shows, each copper site at which methanol is synthesised will become oxidised as a consequence of the synthesis reaction. These oxidised sites constitute in the steady state some 30% of the total surface available initially following reduction (see Table 1), the steady state being maintained by the reactions of CO (16) and H<sub>2</sub> (8) with O(ads).

Oxidation of CO on partially oxidised copper constitutes part of the shift reaction, while TPRS shows that CO is not a product of Cu(I) formate decomposition. The shift reaction, therefore, under methanol synthesis conditions on Cu-ZnO-Al<sub>2</sub>O<sub>3</sub> catalysts does not involve the formate intermediate contrary to previous suggestions (18).

Thus:



The mechanism proposed resembles that found (11, 12, 19) earlier for the synthesis of methanol from CO<sub>2</sub> and H<sub>2</sub> over zinc oxide. This reaction is several orders of magnitude slower than copper-catalysed synthesis and it plays no part in the reaction over Cu/ZnO/Al<sub>2</sub>O<sub>3</sub> catalysts.

#### THE ACTIVE SITE

The experimental results indicate that the active site for methanol synthesis consists of a copper(O) surface atom in close proximity to an oxide surface site. These sites are formed in the first instance by reduction with H<sub>2</sub>, the number of such sites being determined by the H<sub>2</sub>:H<sub>2</sub>O and CO:CO<sub>2</sub> ratios. This view is very similar to that proposed by Okamoto et al (17), following their study of reduced CuO-ZnO surfaces by XPS. From work by Habraken et al (16), and Mesters et al (8), CO reacts faster than H<sub>2</sub> with O(a), but with a significant activation energy, so it is possible that the CO:CO<sub>2</sub> ratio is the more important.

## CONCLUSIONS

Methanol synthesis over Cu-ZnO-Al<sub>2</sub>O<sub>3</sub> catalysts occurs via carbon dioxide hydrogenation on the partially oxidised copper surface. Oxide species may play a direct part in the synthesis by promoting absorption of CO<sub>2</sub> at the copper-oxide interface, reacted CO<sub>2</sub> being replenished via the shift reaction which occurs at different sites and by a different mechanism from methanol synthesis. Overall, CO can react at any oxidic or hydroxidic copper(I) site; methanol synthesis probably occurs at copper(O)/copper(I) sites.

Table 1

Total copper area, during use and copper area following use of a standard Cu/Zn/Al<sub>2</sub>O<sub>3</sub> catalyst and various binary copper/metal oxide catalysts [m<sup>2</sup> per g catalyst charged].  
Standard methanol synthesis conditions.

CATALYST		Cu AREA AFTER REDUCTION	RELATIVE INITIAL ACTIVITY PER g CATALYST	Cu AREA AFTER ACTIVITY TEST	Cu AREA AFTER RE-REDUCTION
Cu-Zn-Al <sub>2</sub> O <sub>3</sub>	60:30:10	32.2	1.0	19.6	29.2
Cu-MgO	60:40	9.0	0.15	7.5	8.6
Cu-MgO	20:80	22.6	0.21	23.4	-
Cu-MgO	40:60	5.9	0.13	6.1	6.4
Cu-MgO	60:40	14.9	0.27	13.0	13.7
Cu-Al <sub>2</sub> O <sub>3</sub>	20:80	11.7	0.45	10.6	-
Cu-Al <sub>2</sub> O <sub>3</sub>	40:60	19.9	0.5	17.2	20.5
Cu-Al <sub>2</sub> O <sub>3</sub>	60:40	12.7	0.40	12.2	11.6
Cu-MnO	20:80	15.6	0.30	14.1	16.0
Cu-MnO	40:60	15.7	0.28	15.4	16.8
Cu-MnO	60:40	23.9	0.38	24.7	26.2

19 March 1984  
SM/L81A14

## REFERENCES

- 1 UK Patent 1159035 (1965).
- 2 H. H. Kung, *Catal. Rev. Sci. Eng.*, 22, 235 (1980)
- 3 K. Klier, *Adv. Catal.*, 31, 243 (1982)
- 4 A. Ya Rozovskii, G. Lim, L. B. Liberov, E. V. Slivinskii, S. M. Loktev, Yu B. Kagan and A. N. Bashkirov., *Kin i Kat* 18 (3), 691, (1977) *Eng. Trans.*
- 5 R. M. Dell, F. S. Stone and P. F. Tiley, *Trans. Farad. Soc.*, 49, 195 (1953).
- 6 J. J. F. Scholten and J. A. Konvalinka, *Trans. Farad. Soc.*, 65, 2465 (1969).
- 7 C. T. Au, J. Breza and M. W. Roberts, *Chem. Phys. Lett.*, 66, 340 (1979)
- 8 C. M. A. M. Mesters, T. J. Vink, O. L. J. Gijzeman and J. W. Geus, *Surface Science*, 135, 428 (1983)
- 9 K. Bauge, D. E. Grinder, T. W. Madey and J. K. Sass, *Surface Science*, 136, 38 (1984)
- 10 D. H. S. Ving and R. J. Madix, *J. Catal.* , 61, 48 (1980).
- 11 M. Bowker, H. Houghton and K. C. Waugh, *J. Chem. Soc., Faraday Trans. 1*, 77, 3023 (1981).
- 12 M. Bowker, H. Houghton and K. C. Waugh, *J. Chem. Soc. Faraday Trans. 1*, 72, 2573 (1982).

REFERENCES (Cont)

- 13 I. E. Wachs and R. J. Madix, *J. Catal.*, 53, 208 (1978).
- 14 W. E. Garner, T. J. Gray and F. S. Stone, *Disc. Farad. Soc.*, 8, 246 (1950).
- 15 E. A. Colbourn and W. C. Mackrodt, Unpublished Results
- 16 F. H. P. M. Habraken, C. M. A. M. Mesters and C. A. Bootsma, *Surface Science* 97 264 (1980)
- 17 Y. Okamoto, K. Fukino, T. Imanaka and S. Teranishi, *J. Phys. Chem.*, 87, 3740 (1983).
- 18 T. van Herwijnen and W. A. de Jong, *J. Catal.*, 63, 83 (1980).
- 19 M. Bowker, J. N. K. Hyland, H. D. Vandervell and K. C. Waugh, 8th Int., Congr. Catal., Berlin (1984).

Figure 1.  $C^m$  activity of outlet gas components as a function of reactant space velocity

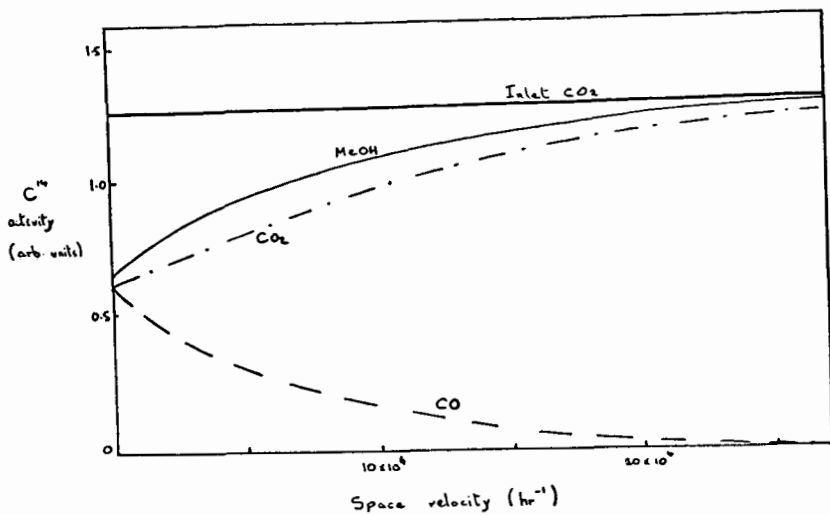


Figure 2. Linear correlation between activity and copper surface area (95% confidence limits) for Cu-ZnO-Al<sub>2</sub>O<sub>3</sub>

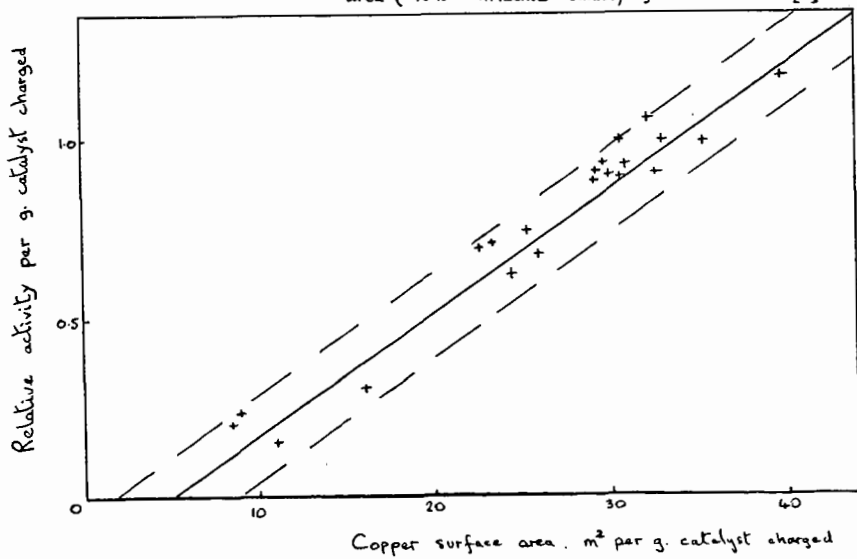


Figure 3 Initial activity of Cu/Zn/Al<sub>2</sub>O<sub>3</sub> catalyts as a function of metallic copper surface area (solid line) compared with binary copper - metal oxide catalyts

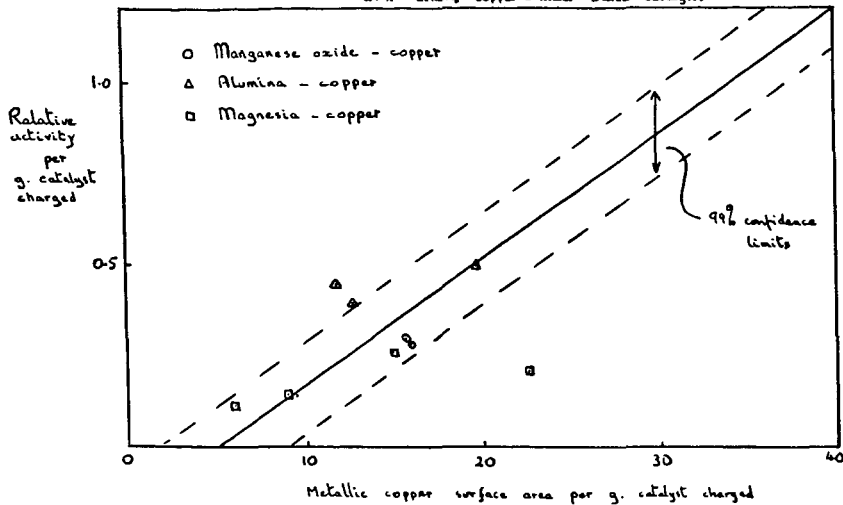
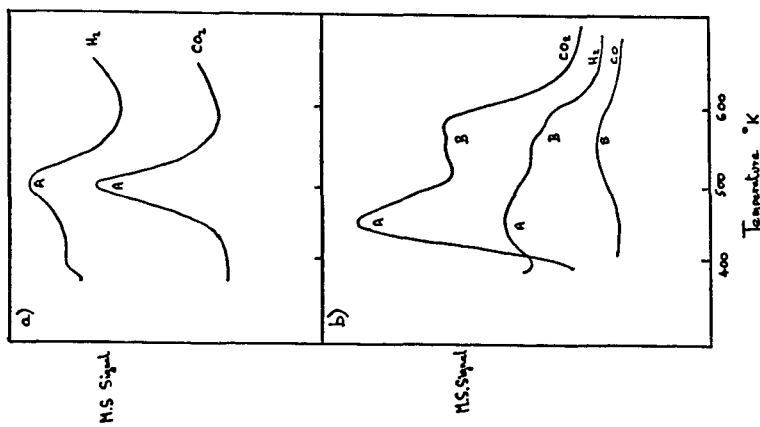


Figure 4



Methanol decomposition on a) unreduced and b) partially reduced Cu-ZnO-Al<sub>2</sub>O<sub>3</sub> catalyst. Peaks A are associated with Cu(I) formate. Peaks B are associated with Zn formate.